THE UNIVERSITY OF MICHIGAN

INDUSTRY PROGRAM OF THE COLLEGE OF ENGINEERING

HETEROGENEOUS NUCLEATION OF CALCIUM SULFATE

Glen C. Smith

A dissertation submitted in partial fulfillment
of the requirements for the degree of
Doctor of Philosophy in the
University of Michigan
Department of Chemical and Metallurgical Engineering
1965

April, 1965

IP-697

To my wife, Carolyn,

my children, and my parents

ACKNOWLEDGEMENTS

It is a pleasure for the author to express his appreciation to the following individuals and organizations for their contributions to the research which was the basis of this dissertation:

The late Dr. Kenneth F. Gordon for his suggestion of the research topic and his strong encouragement of its undertaking.

Professor J. Louis York, chairman of the doctoral committee, for his interest, helpful suggestions, and guidance throughout the course of the research.

Professor Wilbur C. Bigelow for his continual interest in the research topic and for his invaluable instruction in the use of the electron microscope.

The other members of the doctoral committee, Professors Lawrence O. Brockway, Maurice J. Sinnott, and Edwin H. Young, for their helpful advice.

Messrs. Frank Drogosz, William Hungerford, and Robert Smith for their assistance in the design and construction of the electronic equipment and elimination of some of the problems involved in its operation.

Mr. Peter Severn for his skill as a glassblower as demonstrated in the design and construction of the conductivity cells and for his willingness to do the work on short notice.

Messrs. David Johnson and Bernard Schorle, fellow graduate students, for their helpful suggestions, constructive criticisms, and often needed assistance.

My wife, Carolyn, for her patience and encouragement and her help in preparing the first draft of the dissertation.

The Industry Program of the College of Engineering for their excellent work in the final preparation of this dissertation.

The Office of Saline Water of the United States Department of the Interior for their financial support.

TABLE OF CONTENTS

TABLE OF CONTENTS (CONT'D)

LIST OF TABLES

LIST OF FIGURES

LIST OF FIGURES (CONT'D)

NOMENCLATURE

A	Activation energy for nucleation, kcal./mole
a	Surface area, cm^2
C	Solution concentration, gms./1000 gms. soln.
ΔF	Free energy of homogeneous formation, cal.
$\Delta F'$	Free energy of heterogeneous formation, cal.
ΔF_D	Activation energy for diffusion of solute, cal.
f	Heterogeneous nucleation factor
$\bar{H}$	Partial molal enthalpy, cal./mole
$\tilde{H}$	Molal enthalpy, cal./mole
h	Perpendicular distance from origin, cm
h_o	Planck's constant, cal.-sec.
i	Number of molecules in embryo
i^*	Number of molecules in nucleus
J	Nucleation rate, $(cm^2 - min.)^{-1}$
K	Constant (approx.) defined by Equation (15), $(cm^- - min.)^-$
K'	Constant (approx.) = N/K, min.
k	Boltzmann's constant, cal./°K
m_c	Slope of log τ vs. X_c , $°K^3$
m_T	Slope of log τ vs. X_T , °K
N	Number of nuclei formed per unit area in time τ , cm^{-2}
N_o	Avogadro's number, $mole^{-1}$
n^*	Number of molecules in nucleus at the crystal-solution interface

n_s Number of solute molecules in α in contact with the heterogeneous surface per unit area, cm^{-2}

Q Differential heat of solution, cal./mole

R Gas constant, cal./mole-°K

S^j Shape factor defined by Equation (5)

$\bar{S}$ Partial molal entropy, cal./mole-°K

$\tilde{S}$ Molal entropy, cal./mole-°K

T Temperature, °K

V Volume, cm^3

$\tilde{V}$ Molal volume, cm^3/mole

X_c $1/T^3 \log^2(C/C_s)$, $°K^{-3}$

X_T $T_s^2/T\ (T-T_s)^2$, $°K^{-1}$

x Mole fraction of solute in solution

Greek Letters

α_1 Molecule of solute in parent phase

β_i Embryo of precipitating phase containing i molecules

μ Chemical potential of solute, cal./mole

ν Number of ions formed per molecule of solute

σ Crystal-solution interfacial energy, $ergs/cm^2$

τ Nucleation time, min.

Subscripts

i Embryo containing i molecules

i^* Nucleus

s	Saturation
α	Parent phase
β	Precipitating phase

Superscripts

j	Crystalline face

ABSTRACT

Various evaporation processes are currently being used to convert saline water to potable water but they are being hampered by the formation of crystalline deposits on the heating surfaces. Calcium sulfate is one of the most troublesome components of such deposits since the only successful method for preventing its deposition is to halt evaporation before supersaturation is reached. An understanding of the fundamentals involved in the deposition process may be of use in developing other methods of scale prevention.

The heterogeneous nucleation of calcium sulfate was selected for study since it is the first step in the deposition process. Values of the nucleation time, τ , were measured by determining the time required, after the solution had become supersaturated, for a detectable increase in the resistance of the solution which accompanies the precipitation of the solute. This resistance change was measured by electrical conductivity techniques using equipment capable of detecting the precipitation of the order of 10^{-7} grams of calcium sulfate.

Nucleation times were measured for solution concentrations of 1.0, 1.5, 1.8, 1.9, and 2.0 gms of $CaSO_4$ per 1000 gms of solution. The temperature ranges for these concentrations were 128.1° to 130.7°C, 111.7° to 115.7°C, 104.2° to 110.0°C, 101.9° to 107.8°C, and 101.3° to 107.8°C, respectively. Type 316 stainless steel was used as the heterogeneous surface. Electron diffraction patterns of the crystalline

deposits indicate that calcium sulfate hemihydrate was the form which precipitated under these conditions.

Plots of log τ versus $1/T^3\log^2(C/C_s)$ and log τ versus $T_s^2/T(T-T_s)^2$ produced straight lines as predicted by theoretical equations. The slopes of these lines were independent of concentration while the intercepts decreased with a decrease in concentration.

The experimental results show that concentration and temperature have a strong effect on nucleation times. The temperature change required to produce a given change in the nucleation time becomes smaller as the concentration is decreased. For example, to change the nucleation time from 50 to 200 minutes requires a temperature change of 2.8°C at C = 2.0 and 1.0°C at C = 1.0 gms of $CaSO_4$ per 1000 gms of solution.

The solubility of calcium sulfate hemihydrate was determined at 106°, 114°, and 130°C for the solutions used in the nucleation studies. The equivalent conductivity of calcium sulfate was also determined at these same temperatures during the solubility study.

The activation energy for nucleation depends on the degree of supersaturation and was calculated to range from 0.74 to 2.88 kcal/mole for the experimental conditions encountered in this study. The crystal-solution interfacial energy of calcium sulfate hemihydrate was estimated to be 13 ergs/cm^2. The characteristic size of the nuclei and the number of molecules in the nuclei are dependent on the degree of supersaturation and were estimated to range from 11 to 21 Å and from 22 to 144 molecules, respectively.

I. INTRODUCTION

The formation of scale or crystalline deposits from solution onto heat transfer surfaces has long been a problem in such processes as generation of steam, distillation of water, crystallization, and others. Many of the early investigations of this problem were devoted to the development of methods for preventing or minimizing scale formation with little attempt being made to understand the actual scale formation process.[55] Several successful scale prevention techniques were developed from these investigations and have found wide use in boiler water treatment and in the treatment of feed water for small water stills used to provide fresh water on ocean vessels. In recent years there has been an increasing interest in the development of large scale processes for the conversion of saline water to potable water which will be economically competitive with natural fresh water. Many of the methods currently being used are basically evaporation processes and are being hampered by scaling problems. There is a need for fundamental information about the scale formation process since most of the present scale prevention methods are too expensive for large volume conversion plants.[17]

In saline water conversion by evaporation, as is the case in the operation of steam boilers, the three primary components of the scale deposit are calcium carbonate, magnesium hydroxide, and calcium sulfate.[17,39,55] Calcium carbonate and magnesium hydroxide are deposited as the result of a chemical reaction while calcium sulfate

is deposited because its solubility decreases with increasing temperature causing the maximum supersaturation to exist at the heat transfer surface.[4,5,55] At temperatures up to 220°F calcium sulfate constitutes less than five percent of the scale but the percentage begins to increase rapidly as the temperature is increased above this point.[11,28] An inexpensive acid control method has been developed for controlling calcium carbonate and magnesium hydroxide scale[4] but as yet no satisfactory method has been designed for the prevention of calcium sulfate scale other than to halt evaporation before the brine becomes supersaturated with respect to calcium sulfate.[44] The inability to control calcium sulfate deposition places a limit on the maximum operating temperature and the percentage conversion which can be achieved in evaporators, thereby limiting the operating efficiency.[24,44]

It is evident that there is a need for information concerning the many aspects of calcium sulfate scale formation. Information presently available indicates that the first step in scale formation or the deposition of a solid crystalline phase from a supersaturated solution is nucleation, which may be defined as the formation of the first particles, or nuclei, of the new phase when none of this phase existed previously. Nucleation is homogeneous if the supersaturated solution is the only phase present at the sites where nucleation occurs. It is heterogeneous if, in addition to the supersaturated solution, one or more phases, other than the nucleating or precipitating phase, are present at the nucleations sites. Nucleation of

calcium sulfate deposits on heat transfer surfaces is usually heterogenous since these surfaces constitute phases in addition to the supersaturated solution. Therefore, the investigation of the heterogenous nucleation on metallic surfaces is an important step in obtaining fundamental information on the scale deposition process.

Calcium sulfate has three forms which can precipitate from aqueous solution: (1) the dihydrate or gypsum, $CaSO_4 \cdot 2H_2O$, (2) the hemihydrate or plaster of Paris, $CaSO_4 \cdot \frac{1}{2}H_2O$, and (3) the anhydrite, $CaSO_4$. The solubility diagram for the calcium sulfate-water system, reproduced in Figure 1,[55] shows that the dihydrate and the anhydrite are the only two truly stable phases. It is well known, however, that the hemihydrate can exist in metastable equilibrium with its solution for extremely long periods of time and that it is the form which usually precipitates from supersaturated solutions in the temperature range from 100° to 135°C.[39,55] At temperatures above 150°C, however, anhydrite is the form which commonly precipitates. Thus, it would also be of interest in an experimental investigation to know which form of calcium sulfate is being precipitated.

The purpose of this investigation has been to study the heterogeneous nucleation of calcium sulfate from unagitated aqueous solutions on metallic surfaces to determine the effects of the solution concentration and the temperature on the nucleation process. Solution concentrations varied from 1.0 to 2.0 grams of calcium sulfate per 1000 grams of solution and the temperature ranged from 100° to 130°C. The metallic surface used throughout the investigation was type

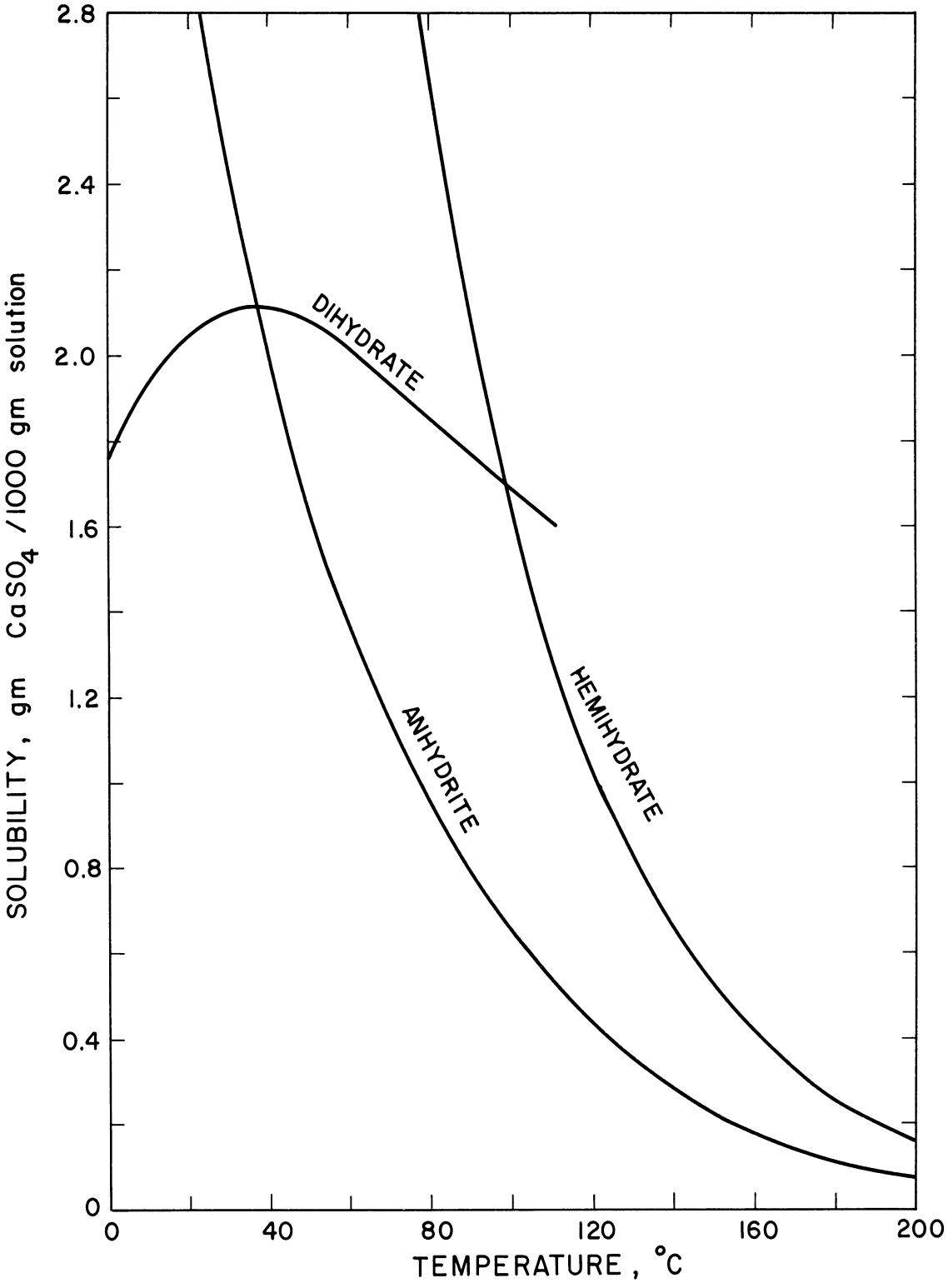

Figure 1. Solubility for the Calcium Sulfate - Water System (Reference 55).

316 stainless steel. The experimental data were analyzed in terms of an appropriately modified version of the kinetic theory of nucleation to obtain values for the activation energy of nucleation, to determine the crystal-solution interfacial energies, and to estimate the approximate size of the nuclei. A few of the scale deposits were examined by electron diffraction and electron microscopy to determine which form of calcium sulfate had precipitated and to obtain information about the shape, size, orientation, and distribution of the crystallites. It was also necessary to determine the solubility of calcium sulfate in the solutions used in this investigation since the scatter of the solubility data obtained from the literature was too great to permit a reasonable interpretation of the experimental results.

II. LITERATURE REVIEW

One of the earliest theories of nucleation from solution was suggested by Ostwald[54] who stated that a solution could be supersaturated into two regions: (1) a metastable region where crystal growth could occur but where nucleation was impossible, and (2) a labile region, at a higher concentration, where spontaneous nucleation could take place as well as crystal growth. Miers[46] and de Coppet[14] extended this concept by suggesting that there was a definite and reproducible boundary between the metastable and labile regions. This boundary was called a supersolubility curve and was approximately parallel to the solubility curve but at higher concentrations. Although this supersolubility theory has had some recent experimental support,[1,13,61] it has come under criticism for its inability to explain nucleation which occurs in the metastable region.[2,15,68,79] One of the recent supporters[13] admits that nucleation might take place in the metastable region at a very slow rate, and deCoppet[14] noted that the supersolubility curve moved closer to the solubility curve as the time of observation for nuclei was increased. Further evidence that the supersolubility concept is not the complete answer to understanding nucleation is provided by the fact that such variables as agitation,[26,33] mechanical shock,[83] and the presence of insoluble impurities[27] cause nucleation to occur well into the metastable region. In recent years, therefore, the kinetic theory of nucleation has all but replaced the supersolubility concept.

Only a brief summary of the theory is presented here since a detailed derivation of the theory is given in the next section.

According to the kinetic theory, the formation of a nucleus is thought to occur by the stepwise combination of solute molecules into molecular aggregates since the probability of the simultaneous collision of the number of molecules required for a nucleus is extremely low. As a result of the statistical distribution of energy within the bulk of the solution there will be localized areas whose energy level will be sufficiently above the average value to provide the energy required for nucleation. Based upon these concepts, equations have been derived which predict that the nucleation rate is strongly dependent on the energy required for the nucleus formation. Since the nucleation energy is related to the degree of supersaturation these equations also predict that the nucleation rate is strongly dependent on the degree of supersaturation. These theoretical equations have been tested and have shown good agreement with experimental data for many systems. Because of the strong dependence of the nucleation rate on supersaturation it is easy to see why some investigators accept the supersolubility concept, but at the same time there is no theoretical reason to believe that nucleation will not occur at any degree of supersaturation. The presence of insoluble impurities would be expected to increase the rate of nucleation since they would, in general, decrease the energy required for nucleation because of surface energy effects. Other influences, such as agitation and mechanical shock mentioned earlier, would also tend to

increase the nucleation rate by causing energy increases in localized areas. Therefore, the kinetic nucleation theory has been experimentally verified, gives a practical interpretation of the supersolubility theory, and is able to explain some of the discrepancies found in this latter theory.

Very little data is available in the literature on the nucleation of calcium sulfate from solution although several articles have appeared on the rate of crystallization.[43,47,48,49,50,64,66] Deryabina[16] and Mutaftschiew[52] studied the homogeneous nucleation of the dihydrate of calcium sulfate from aqueous solutions by mixing salt solutions to obtain supersaturation. Although the temperatures of their investigations are not known they presumably were in the neighborhood of room temperature since they studied the nucleation of the dihydrate. Moriyama[50] studied the rate of growth of dihydrate crystals at 20° to 35°C by a conductometric technique and noted an induction period or time lag before crystal growth began. However, due to the method of preparing the supersaturated solutions, he was unable to measure the length of the induction period since he could not determine when supersaturation was achieved. Schierholtz[62] studied the rate of crystallization of the dihydrate at 25°C by a chemical analysis technique and also reported the occurrence of a time lag before crystallization began. Van Hook[73] reports some unreferenced data on induction periods for the nucleation of calcium sulfate dihytrate at 25°C. Although some work has been done on the nucleation of the dihydrate little or no work has been done on the nucleation of calcium sulfate hemihydrate.

The earliest method of studying nucleation consisted of observing the formation of the nuclei with the unaided eye. More recent methods have consisted of detecting the nuclei microscopically[80] or of observing some property of the solution which is strongly affected by the formation of nuclei such as electrical conductivity[2,3,9,59,70] or turbidity.[38,77] Of these methods of investigation, only direct observation and measurement of electrical conductivity are applicable to studies of heterogeneous nucleation on a surface. The turbidity method is useful primarily for detecting nucleation which occurs within the bulk of the solution. The method of direct observation has the disadvantage of being limited to the detection of nucleation on small areas of surface since the high magnifications required to detect the nuclei in their early stages of growth limit the amount of area that can be observed. The electrical conductivity method can detect nucleation which occurs anywhere in the system, and with modern electronic equipment it can be extremely sensitive.

A search of the literature has revealed that no data are available on the nucleation of calcium sulfate in the temperature range of 100° to 130°C, even though there is considerable need for such information. The kinetic theory of nucleation shows that the degree of supersaturation is by far the most important variable affecting the rate of nucleation and is the variable which was selected for study in this investigation. Although other variables, such as agitation, mechanical shock, etc., might have some influence on the nucleation process they were excluded from this study because a knowledge of their

effect on the energy distribution within the solution is required to incorporate them into the equations derived from nucleation theory. The heterogeneous nucleation of calcium sulfate was detected by measuring the electrical resistance of the supersaturated solutions since this method is quite sensitive and is one of the few methods suitable for the study of heterogeneous nucleation.

III. THEORETICAL DEVELOPMENT

The first complete theory of nucleation was developed by Volmer and Weber[76] for the homogeneous nucleation of liquids from vapors. This theory was subsequently modified by Becker and Doering,[6] and this modified version was then extended by Volmer[75] to the case of heterogeneous nucleation of liquids from vapors. Recently this theory has been modified to cover nucleation from condensed systems by Turnbull and Fisher[72] for homogeneous nucleation and by Turnbull[69] for heterogenous nucleation. A brief description of the essential features of the current nucleation theory, based largely on the treatment by Dufour and Defay,[18] is presented here since this theory will be used in the analysis of the experimental results. Additional information on the nucleation theory can be found in several recently published reviews.[18,20,29,30,51,71,73]

The precursors of the crystals precipitating from a supersaturated solution are presumably embryos formed by the stepwise combination of solute molecules according to the scheme

$$\begin{aligned} \alpha_1 + \alpha_1 &= \beta_2 \\ \beta_2 + \alpha_1 &= \beta_3 \\ &\cdots\cdots \\ \beta_{i-1} + \alpha_1 &= \beta_i \end{aligned} \qquad (1)$$

where α_1 represents a molecule of the solute in the parent α phase and β_i is an embryo, containing i molecules, of the precipitating β

phase. This scheme is proposed since the probability of i solute molecules colliding simultaneously is extremely low.(71)

By assuming the embryos to have the same properties as the crystalline phase the free energy required to form an embryo homogeneously may be calculated as

$$\Delta F_i = \frac{i(\mu_\beta - \mu_\alpha)}{N_o} + \sum_j a_i^j \sigma_i^j \qquad (2)$$

where ΔF_i is the free energy of formation, i is the number of molecules in the embryo, N_o is Avogadro's number, μ_β and μ_α are the chemical potentials of the solute in the β and α phases, respectively, and a_i^j and σ_i^j are the surface area and the solution-crystal interfacial energy, respectively, of the j-th face of a crystal embryo containing i molecules. According to Gibbs (Reference 73, pp. 58-65) a crystal embryo will form in such a way that

$$\frac{\sigma_i^1}{h_i^1} = \frac{\sigma_i^2}{h_i^2} = ... = \frac{\sigma_i^j}{h_i^j} = \text{constant} \qquad (3)$$

where h_i^j is the perpendicular distance from the point of orgin of the embryo to the j-th face of an embryo containing i molecules. Using Equation (3)

$$\sum_j a_i^j \sigma_i^j = \sum_j \frac{\sigma_i^j}{h_i^j} a_i^j h_i^j = \frac{\sigma_i^j}{h_i^j} \sum_j a_i^j h_i^j = 3 V_i \frac{\sigma_i^j}{h_i^j} \qquad (4)$$

where V_i is the volume of the embryo. A shape factor is introduced as defined by the relation

$$V_i = \frac{1}{3} S^j (h_i^j)^3 \tag{5}$$

where the shape factor, S^j, depends on the shape of the crystal and the choice of face j. The volume of the embryo is related to the molal volume of the β phase by the expression

$$V_i = i \frac{\tilde{V}_\beta}{N_o} \tag{6}$$

where $\tilde{V}_\beta$ is the molal volume. Combining Equations (2), (4), (5), and (6) yields

$$\Delta F_i = \frac{S^j (h_i^j)^3 (\mu_\beta - \mu_\alpha)}{3 \tilde{V}_\beta} + S^j \sigma_i^j (h_i^j)^2 \tag{7}$$

Since $\mu_\beta - \mu_\alpha < 0$ in order for the β phase to spontaneously form in the presence of the α phase, a plot of ΔF_i versus h_i^j will go through a maximum. Differentiating Equation (7) with respect to h_i^j and setting it equal to zero yields the coordinates of this maximum point as

$$\Delta F_{i*} = \frac{4 S^j (\sigma^j)^3 \tilde{V}_\beta^2}{3(\mu_\beta - \mu_\alpha)^2} \tag{8}$$

$$h_{i*}^j = - \frac{2 \sigma^j \tilde{V}_\beta}{(\mu_\beta - \mu_\alpha)} \tag{9}$$

where σ_i^j is assumed to be independent of i or $\sigma_i^j = \sigma^j$. Combining Equations (5), (6), and (9) yields

$$i* = - \frac{8 N_o S^j (\sigma^j)^3 \tilde{V}_\beta^2}{3(\mu_\beta - \mu_\alpha)^3} \tag{10}$$

where i^* is the minimum number of molecules which an embryo must possess to be considered a stable nucleus. On the average, larger embryos will continue to increase in size and smaller embryos will redissolve since each of these processes results in a decrease in free energy.

The derivation of the theoretical equations to this point has been for the case of homogeneous nucleation or nucleation within the bulk of the solution. Extension of this treatment to heterogeneous nucleation requires only a modification of the expression for the free energy required for the formation of a nucleus. This effect may be expressed as

$$\Delta F'_{i^*} = f \, \Delta F_{i^*} \tag{11}$$

where $\Delta F'_{i^*}$ is the free energy of formation of a nucleus on a heterogeneous surface and $f \leq 1$ is the heterogeneous nucleation factor. The calculation of f requires information on the shape and orientation of the nucleus and the crystal-solution, crystal-surface, and surface-solution interfacial energies. Fletcher[21] derived an expression for f, expressed in terms of the contact angle between the nucleus and the heterogeneous surface, for the case of nuclei shaped like spherical segments. Values of f for other shapes can also be calculated provided the necessary information, mentioned above, is available.

The rate of heterogeneous nucleation may be defined as the number of nuclei formed per unit time per unit area of the heterogeneous surface. Stated another way, the heterogeneous nucleation rate, J, is the net frequency, per unit area of the heterogeneous surface, of the process

$$\beta_{i^*-1} + \alpha_1 = \beta_{i^*} \tag{12}$$

Turnbull[69] applied the absolute reaction rate theory to this expression and obtained the following quantitative expression for J

$$J = (x-x_s)\, n^* n_s \left(\frac{kT}{h_o}\right) \left(\frac{S^j \sigma^j}{\pi k T}\right)^{1/2} \left(\frac{\tilde{V}_\beta}{9N_o S^j}\right)^{1/3} \exp\left[\frac{-(f\Delta F_{i^*}+\Delta F_D)}{kT}\right] \quad (13)$$

where x and x_s are the mole fractions of solute in the supersaturated and saturated solutions, respectively, n^* is the number of molecules in the surface of the nucleus in contact with the solution, n_s is the number of solute molecules in contact with the heterogeneous surface per unit area, k is Boltzmann's constant, h_o is Planck's constant, T is the absolute temperature, ΔF_D is the activation energy for the diffusion of the solute through the solution, and the rest of the terms are as defined earlier. Since the temperature interval over which the rate of nucleation can be conveniently measured is usually small, many of these variables may be assumed constant for a given solution concentration, and Equation (13) may be written more simply as

$$J = K \exp(-f\Delta F_{i^*}/kT) \quad (14)$$

where

$$K = (x-x_s)\, n^* n_s \left(\frac{kT}{h_o}\right) \left(\frac{S^j \sigma^j}{\pi kT}\right)^{1/2} \left(\frac{\tilde{V}_\beta}{9N_o S^j}\right)^{1/3} \exp\left(-\frac{\Delta F_D}{kT}\right) \quad (15)$$

Combining Equations (8) and (14) yields

$$J = K \exp -\left[\frac{4fS^j(\sigma^j)^3 \tilde{V}_\beta^2}{3kT(\mu_\beta-\mu_\alpha)^2}\right] \quad (16)$$

Equation (16) may be put into a more useful form by expressing the difference in chemical potentials of the solute in the two phases in terms of physically measurable variables. If the solution was saturated at the temperature T the chemical potential of the solute in the two phases would be equal and may be expressed as

$$\mu_\beta = \mu_\alpha\Big|_{C=C_s} \tag{17}$$

The difference in chemical potentials for a supersaturated solution at the temperature T may be expressed as

$$\mu_\beta - \mu_\alpha = \mu_\alpha\Big|_{C=C_s} - \mu_\alpha\Big|_{C=C} \tag{18}$$

Combining Equation (18) with the thermodynamic expression for the isothermal change of chemical potential with change in concentration yields

$$\mu_\beta - \mu_\alpha = -\nu RT \ln (C/C_s) \tag{19}$$

when it is assumed that the activity coefficients are equal for the two concentrations. In Equation (19) ν is the number of ions formed from each molecule of solute, C is the solution concentration, and C_s is the saturated concentration at the temperature T.

Based on thermodynamic definitions, the chemical potential difference may also be expressed in the following convenient form

$$\mu_\beta - \mu_\alpha = (\tilde{H}_\beta - \bar{H}_\alpha) - T(\tilde{S}_\beta - \bar{S}_\alpha) \tag{20}$$

where $\tilde{H}_\beta$ and $\tilde{S}_\beta$ are the molal enthalpy and entropy, respectively,

of the pure β phase, and $\bar{H}_\alpha$ and $\bar{S}_\alpha$ are the partial molal enthalpy and entropy, respectively, of the solute in the α phase. If the temperature of the solution is changed, at constant composition, to the saturation temperature, T_s, the chemical potentials would be equal and Equation (20) would yield

$$T_s(\tilde{S}_\beta - \bar{S}_\alpha)\Big|_{T=T_s} = (\tilde{H}_\beta - \bar{H}_\alpha)\Big|_{T=T_s} = -Q \qquad (21)$$

where Q is the differential heat of solution.[36,40] Combining Equations (20) and (21) and assuming the heat of solution and the difference in partial molal entropies to be constant yields

$$\mu_\beta - \mu_\alpha = Q\left(\frac{T-T_s}{T_s}\right) \qquad (22)$$

where T_s is the saturation temperature. Substituting Equations (19) and (22) into Equation (16) results in

$$J = K \exp\left[\frac{-4f N_o S^j (\sigma^j)^3 \tilde{V}_\beta^2}{3\nu^2 R^3 T^3 \ln^2(C/C_s)}\right] \qquad (23)$$

or

$$J = K \exp\left[\frac{-4f N_o S^j (\sigma^j)^3 \tilde{V}_\beta^2 T_s^2}{3RT\, Q^2 (T-T_s)^2}\right] \qquad (24)$$

where $R = N_o K$ is the gas constant.

Although the nucleation equations yield values for the nucleation rate these same equations may be used to correlate induction periods

or so-called nucleation times.[20,73] The nucleation time, τ, may be defined as the time required to detect N nuclei per unit area of the heterogeneous surface so that

$$\tau = N/J \tag{25}$$

Substituting Equation (25) into Equations (23) and (24) and taking logarithms produces the relations

$$\log \tau = \log K' + \left[\frac{4fN_o S^j (\sigma^j)^3 \tilde{V}_\beta^2}{3(2.303R)^3 \nu^2}\right] \frac{1}{T^3 \log^2(C/C_s)} \tag{26}$$

or

$$\log \tau = \log K' + \left[\frac{4fN_o S^j (\sigma^j)^3 \tilde{V}_\beta^2}{3(2.303R)Q^2}\right] \frac{T_s^2}{T(T-T_s)^2} \tag{27}$$

where $K' = N/K$.

Over small temperature ranges the terms inside of the brackets remain essentially constant so that plots of $\log\tau$ versus $X_c \equiv 1/T^3\log^2(C/C_s)$ and $\log\tau$ versus $X_T \equiv T_s^2/T(T-T_s)^2$ should yield straight lines. If the slopes of such lines are denoted by m_c and m_T, respectively, it can be seen from Equations (26) and (27) that

$$m_c = \left[\frac{4fN_o S^j (\sigma^j)^3 \tilde{V}_\beta^2}{3(2.303R)^3 \nu^2}\right] \tag{28}$$

and

$$m_T = \left[\frac{4fN_o S^j (\sigma^j)^3 \tilde{V}_\beta^2}{3(2.303R)Q^2}\right] \tag{29}$$

These slopes may be used to calculate the crystal-solution interfacial energy, the activation energy for nucleation, the number of molecules in the nucleus, and the approximate size of the nucleus. The interfacial energy may be calculated by the relations

$$\sigma^j = 2.303R \left[\frac{3m_c \nu^2}{4fN_o S^j \tilde{V}_\beta^2} \right]^{1/3} \tag{30}$$

or

$$\sigma^j = \left[\frac{3(2.303R)Q^2 m_T}{4fN_o S^j \tilde{V}_\beta^2} \right]^{1/3} \tag{31}$$

The number of molecules in the nucleus may be determined by combining Equations (10), (19), and (30) and Equations (10), (22), and (31) to yield

$$i^* = \frac{2m_c}{\nu f T^3 \log^3(C/C_s)} = \frac{2m_c}{\nu f} (TX_c)^{3/2} \tag{32}$$

or

$$i^* = -\frac{2(2.303R)m_T}{fQ} \left(\frac{T_s}{T-T_s} \right)^3 = -\frac{2(2.303R)m_T}{fQ} (TX_T)^{3/2} \tag{33}$$

The activation energy, A , is defined as $A = f\Delta F_{i^*} N_o$ [59,74] and may be calculated by combining Equation (8) with Equations (19) and (30) or Equations (22) and (31) to give

$$A = \frac{2.303R\, m_C}{T^2 \log^2(C/C_s)} = 2.303RT\, m_c X_c \tag{34}$$

or

$$A = \frac{2.303RT_s^2 m_T}{(T-T_s)^2} = 2.303RT\, m_T X_T \qquad (35)$$

Lastly, the size of the nucleus can be calculated from the equations obtained by combining Equation (9) with (19) and (30) or (22) and (31).

$$h_{i*}^j = \left[\frac{6\tilde{V}_\beta m_c}{\nu f N_o S^j}\right]^{1/3} \frac{1}{T \log(C/C_s)} = \left[\frac{6\tilde{V}_\beta m_c}{\nu f N_o S^j}\right]^{1/3} (TX_c)^{1/2} \qquad (36)$$

or

$$h_{i*}^j = \left[\frac{-6(2.303R)\tilde{V}_\beta m_T}{f N_o S^j Q}\right]^{1/3} \frac{T_s}{T-T_s} = \left[\frac{-6(2.303R)\tilde{V}_\beta m_T}{f N_o S\, Q^j}\right]^{1/3} (TX_T)^{1/2} \qquad (37)$$

It is of interest at this point to consider the relation between Equations (19) and (22) for the difference in the chemical potentials of the solute in the two phases. By equating the two expressions and using the definitions for X_c and X_T it can be shown that

$$X_c = \left(\frac{2.303R\nu}{Q}\right)^2 X_T \qquad (38)$$

Using the definitions for m_c and m_T yields the relation

$$m_c = \left(\frac{Q}{2.303R\nu}\right)^2 m_T \qquad (39)$$

Combination of Equations (38) and (39) yields

$$m_c X_c = m_T X_T \qquad (40)$$

which means that plotting $\log\tau$ versus X_c or X_T will yield the same results and the choice of which form to use is arbitrary.

It is apparent from this theoretical development that the determination of nucleation times at different levels of supersaturation can be useful in understanding the effects of temperature and concentration on the nucleation process. The equipment used for determining the nucleation times of supersaturated calcium sulfate solutions is described in the following section.

IV. EXPERIMENTAL EQUIPMENT

The change in the electrical resistance of a solution which accompanies the concentration decrease caused by precipitation of the solute was used to study the heterogeneous nucleation of calcium sulfate. The equipment consisted basically of a set of conductivity cells, a constant temperature bath, and electronic components necessary to detect changes in resistance. This equipment is described here to the extent necessary for an understanding of the experimental procedures, but a more detailed description of some of the equipment is given in Appendix D.

1. Conductivity Cells

The conductivity cells, shown schematically in Figure 2, were constructed of Pyrex glass and were designed to have a resistance of approximately 4,000 ohms when filled with a 0.2% by weight calcium sulfate solution at 120°C. The electrodes were platinum foil 0.001 inches thick, 10 mm wide, and 30 mm long, and were embedded in the glass wall of the cells by the method described by Campbell.[7] Electrical contact was made with these electrodes by fusing 30 gage (0.010 in. diam.) platinum wire to the platinum foil and bringing the platinum wire out through glass side arms. Ground glass joints were used so the cells could be cleaned and filled easily and so the stainless steel samples could be easily inserted and removed.

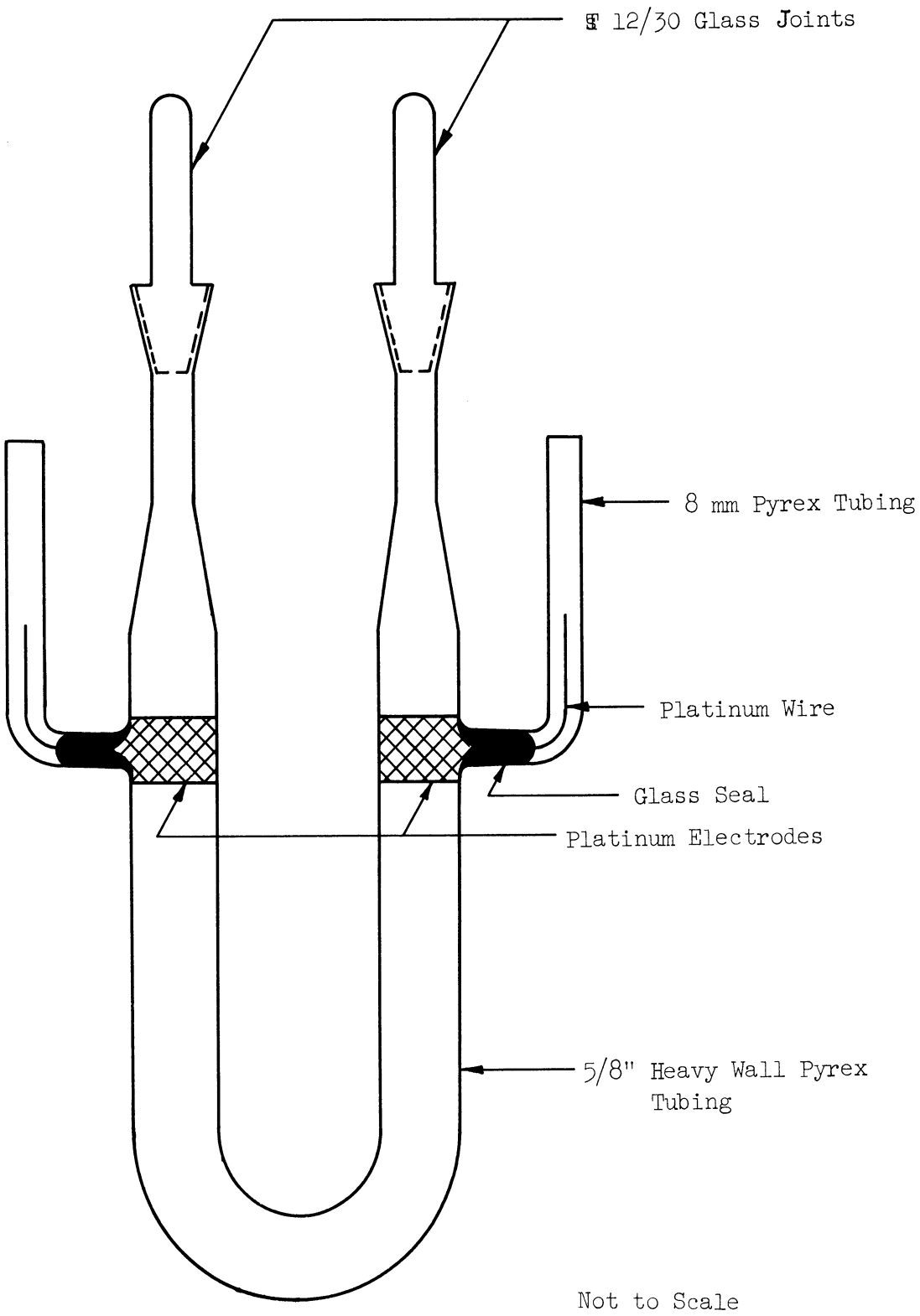

Figure 2. Sketch of Conductivity Cell.

2. Constant Temperature Bath

The constant temperature bath had to provide a very close temperature control since small temperature fluctuations would have caused changes in the resistance of the solution sufficient to overshadow the changes due to nucleation. The bath consisted of an 18" x 18" x 14" stainless steel container completely surrounded by 4 inches of air cell insulation. The bath medium used was "Ucon" type 50-HB-280X, a commercial heat-transfer fluid manufactured by Union Carbide Chemicals Company. This fluid was selected because its resistance to oxidation and its low vapor pressure allowed it to be used in an open bath. It was also water-soluble enabling it to be easily rinsed from the conductivity cells. Vigorous agitation was provided by a 4 inch propeller placed approximately in the center of the bath and rotated at approximately 1500 rpm. The heat necessary to maintain the temperature was supplied by a 1000-watt tubular heater placed in the bottom of the bath and a 450-watt knife heater placed through the top cover, with the power to the heaters being obtained from Variacs. The 1000-watt heater was adjusted manually while the 450-watt heater was controlled automatically by an electronic relay. A detailed description of the heater and control circuit is given in Appendix D. The sensing element was a spiral bimetallic thermoregulator manufactured by the American Instrument Company with a reported sensitivity of 0.005°C. The bath temperature was indicated by calibrated mercury thermometers while temperature fluctuations were indicated by a Beckmann differential thermometer which could be easily

read to 0.001°C. The bath performed very satisfactorily with the temperature change being less than 0.005°C for most of the experimental runs.

3. Electronic Components

The electronic equipment was the most important part of the experimental apparatus since it had to provide the high sensitivity necessary to detect small changes in the concentration of the solution. The overall arrangement of the electronic components is shown schematically in Figure 3, and may be classified into four sections: (1) the bridge power supply, (2) the bridge, (3) the detector, and (4) the ground circuit. This system was capable of detecting changes in the output voltage of the bridge of the order of 10^{-5} volts which corresponded to the precipitation of the order of 10^{-7} grams of calcium sulfate.

The power supply for the bridge was a Hewlett-Packard model 200CD audio oscillator which was operated at a frequency of 1000 cycles per second. The supply voltage depended to a small extent on the cell resistance but was approximately 17 volts peak-to-peak or 6.0 volts rms.

The bridge was composed of the conductivity cell (R_c), three precision decade resistors (R_1, R_2, R_4), a variable precision air capacitor (C_4), and a fixed capacitor (C_1), as shown in Figure 3. The capacitors were necessary to balance out the inherent capacitance of the conductivity cells. The high sensitivity of the detector required shielding of the bridge in order to minimize the interference caused by the pickup of stray 60 cycle signals. This was achieved by shielding each of the bridge components except the fixed capacitor, using shielded wire for all connections, and grounding all shields. The

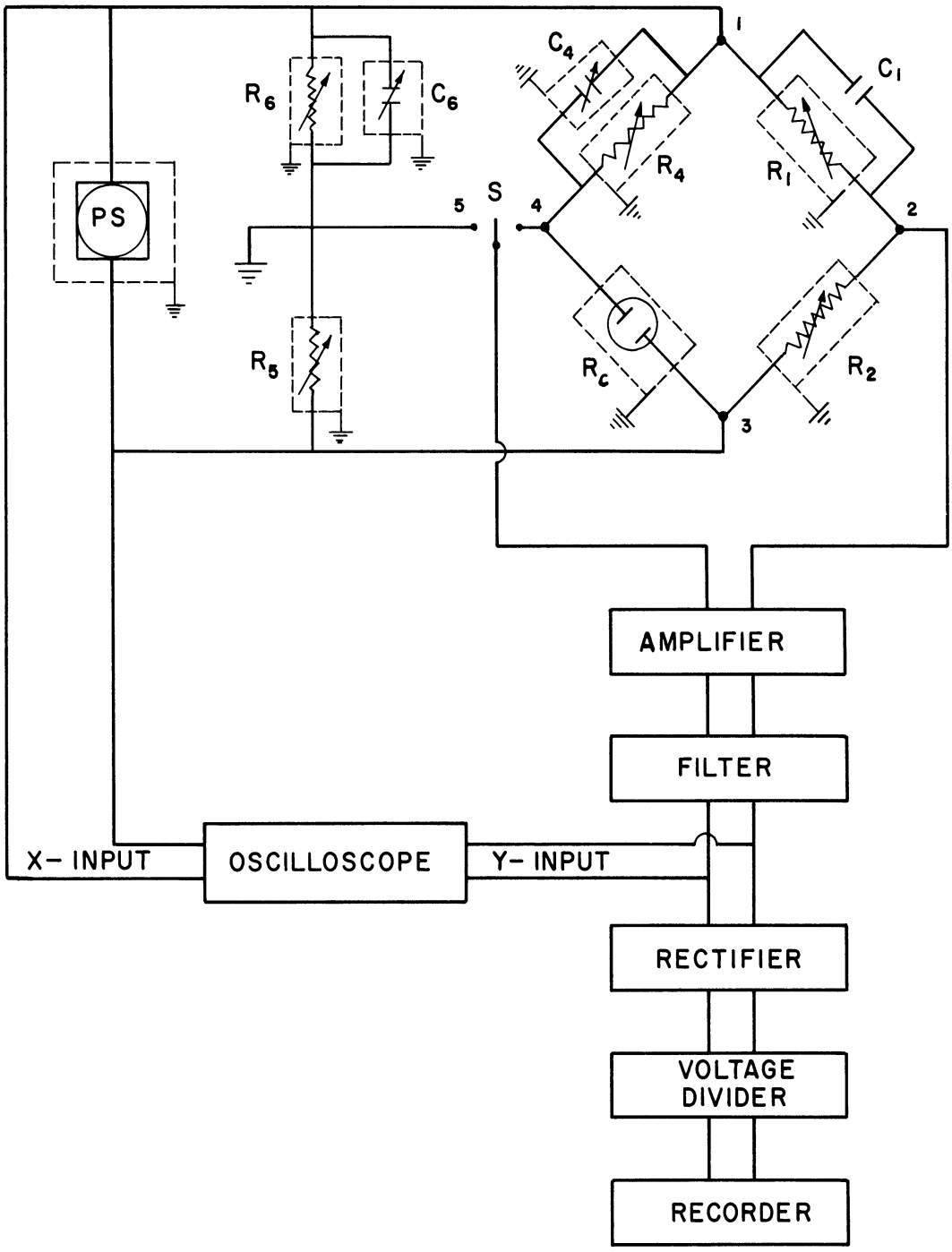

See Appendix F for description of components.

Figure 3. Schematic Diagram Showing Connection of Electronic Components.

stainless steel bath container provided adequate shielding for the conductivity cells.

The detector consisted of an electronic amplifier, electronic filter, oscilloscope, rectifier, voltage divider, and recorder connected together as shown schematically in Figure 3. The two-stage amplifier was designed to be non-linear to help damp out 60 cycle pick-up and had a peak gain at the bridge signal frequency. The filter is a single-stage amplifier using negative feedback through a parallel-T network tuned to 1000 cps, and provided additional amplification of the 1000 cps signal while greatly reducing any 60 cycle signal picked up by the bridge. The amplifier-filter combination provided an over-all voltage gain of about 3,000 at 1000 cps, 10 at 60 cps, and 20 at 20,000 cps and, thereby, provided a fairly clean 1000 cps output signal. The rectifier provided some amplification but served primarily to convert the amplified and filtered bridge output voltage to a direct current voltage with no detectable ripple when check by the oscilloscope at 1 millivolt/cm sensitivity. The total amplification of the amplifier-filter-rectifier combination was approximately 4,000 referring the DC output voltage to the peak-to-peak value of the 1000 cps input voltage. Circuit diagrams and further discussion of the amplifier, filter and rectifier are presented in Appendix D. The output voltage from the rectifier was of the order of volts and was reduced by a factor of 1000 in the voltage divider, which had a total resistance of 10,000 ohms, before it was recorded on a potentiometric millivolt strip-chart recorder. The oscilloscope was necessary to determine if

the bridge output voltage was due to unbalance in the resistance or capacitance or both since this information could not be provided by the output voltage of the rectifier. This phase-sensitive indication of the unbalance was obtained by supplying the X-input of the oscilloscope from the bridge oscillator and the Y-input from the filter in order to produce a Lissajous pattern.[65] The detector was capable of detecting changes in the output voltage of the bridge of the order of 10^{-5} volts. Power to the electronic components, except for the battery powered filter, was supplied by a constant voltage transformer to eliminate appreciable changes in the recorded voltage which might be caused by line voltage fluctuations. When the conductivity cell was replaced by a fixed precision resistor no detectable change was observed in the recorded voltage over a period of three and a half hours which indicated that the detector was quite stable.

The ground circuit consisted of two shielded decade resistors (R_5, R_6) and a shielded variable air capacitor (C_6). This circuit was necessary to minimize errors in the bridge readings which might be caused by stray capacitances, especially between the detector and ground.[41,63,65] In use the bridge was first balanced by adjusting R_4 and C_4 with the switch S in position 4, and then again by adjusting R_6 and C_6 with the switch in position 5. This was repeated until no output signal was obtained with the switch in either position. At this time the bridge was balanced with points 2 and 4 at ground potential, eliminating the effects of stray detector to ground capacitances.

V. EXPERIMENTAL PROCEDURES

The equipment described in the preceding section was used to measure nucleation times for the heterogeneous nucleation of calcium sulfate from aqueous solution onto Type 316 stainless steel. The procedures used to obtain the experimental data, a discussion of the uncertainties in the measured quantities, and some of the experimental difficulties are described here.

1. Preparation of Solution

The solution preparation system was designed to provide solutions reasonably free from undissolved impurities since such impurities could act as nucleation sites. A schematic diagram of this system is given in Figure 4. The solution was prepared in the mixing vessel by dissolving analytical reagent grade calcium sulfate in double-distilled water with agitation provided by a magnetic stirrer. After being agitated for about twenty-four hours the undissolved calcium sulfate was allowed to settle and the supernatant solution was transferred to the solution reservoir through a Gelman Instrument Company, Type GM-8, cellulose acetate, membrane filter which had a nominal pore size of 0.2 microns. Double-distilled water was then passed through the filter into the solution reservoir to rinse the calcium sulfate solution from the lines and to adjust the concentration of the solution in the reservoir to the desired value. The vent at A was used to exhaust air from the lines ahead of the filter since it is very difficult to force air through the membrane filter once it has been wetted. Stopcock B was used

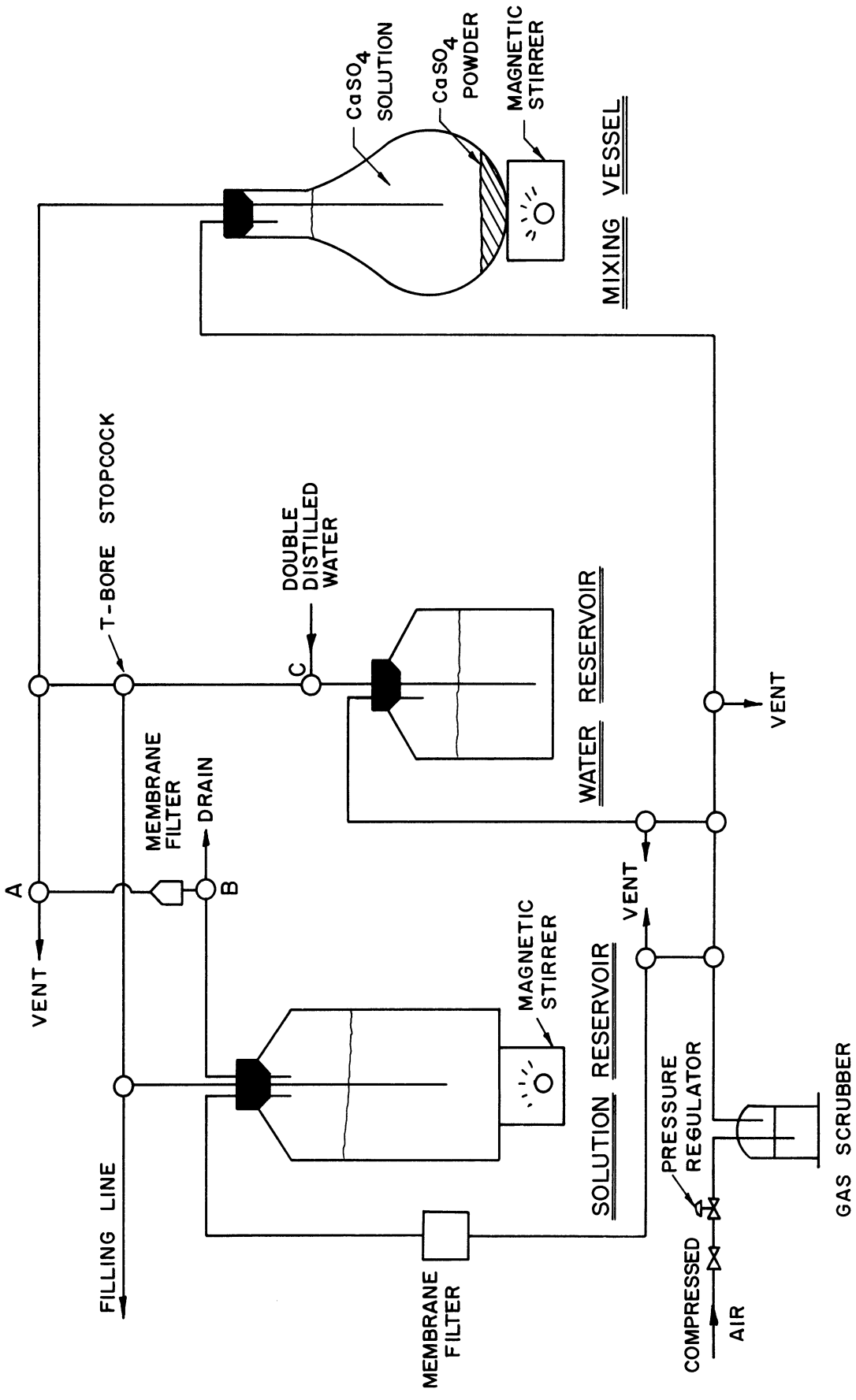

Figure 4. Schematic Diagram of Solution Preparation System.

to isolate the solution reservoir when it became necessary to change the solution filter and to provide a discharge port so the filtered solution line could be thoroughly rinsed with filtered water after the filter had been changed. The water reservoir was filled through stopcock C. The solution in the reservoir was thoroughly agitated by a magnetic stirrer to eliminate concentration gradients before it was transferred to the conductivity cells through the filling line. The movement of solution and water through the system was achieved by compressed air which was first passed through a gas scrubber containing double-distilled water to remove large dust particles. The compressed air used to force the solution from the reservoir was filtered further by passing it through a membrane filter like the one used to filter the solution. The air was controlled by a manifold designed so that each vessel could be pressurized or vented independently of the others. The vessels and stopcocks were made of Pyrex glass. All transfer lines which came in contact with solution, double-distilled water, or filtered air were made of Pyrex glass and Tygon tubing, while all other air lines were of rubber tubing. The filter holder for the solution filter was made of stainless steel while the holder for the air filter was made of aluminum.

Solution concentrations were determined by titration with an aqueous solution of disodium versenate (the disodium salt of ethylenediaminetetraacetic acid, sometimes called EDTA) and magnesium chloride. The versenate solution was standardized against a calcium

chloride solution prepared by dissolving a carefully weighed sample of dried reagent grade calcium carbonate in a small amount of dilute hydrochloric acid and diluting to the desired volume with double-distilled water. A buffer solution of ammonium chloride in ammonium hydroxide was used in the titrations to adjust the pH . The end point indicator was Eriochrome Black T dissolved in methanol.[81]

2. Preparation of Metal Surfaces

Type 316 stainless steel was used as the heterogeneous surface throughout this investigation since it would not react with the aqueous solutions. This requirement was necessary since such reactions might cause changes in the electrical resistance of the solution which could overshadow the effects due to nucleation. Initial experiments with brass and copper samples indicated that these materials were unsuitable since they tarnished visibly when placed in distilled water at room temperature for a few hours.

The metal samples were prepared by abrading 3/16 inch wide strips of 22 gage (0.025 in. thick) Type 316 stainless steel with 600 grade metallographic paper. These strips were then cut into 3/16 inch squares and sharp burrs or edges were removed with metallographic paper. These samples were cleaned ultrasonically in toluene, then in acetone, and finally in double-distilled water, after which they were stored in double-distilled water until used. This cleaning procedure was selected after making an electron microscopic examination of samples cleaned by different methods. An electron micrograph of a sample cleaned by this technique is reproduced in Figure 5.

Figure 5. Electron Micrograph of Type 316 Stainless Steel Sample, x 9,700.

3. Determination of Nucleation Time

The cells were thoroughly cleaned before filling to minimize contamination by dust particles. The ground glass joints were first washed with kerosene to remove the silicone stopcock grease which was used to seal the joints. The cells were then thoroughly cleaned in a detergent solution to remove the kerosene and bath oil, rinsed in tap water, washed again in a clean detergent solution, and then rinsed successively with tap water, distilled water, and double-distilled water. These cells were then mounted in an inverted position and steamed for one hour with steam generated by boiling double-distilled water. The cells were immediately turned upright and filled from the solution reservoir by forcing 250-300 milliliters of solution through the cells by air pressure. The stainless steel sample was removed from its storage place, rinsed with double-distilled water, and placed into the cell as soon as possible after the solution began flowing into the cell. While the cell was being filled, the glass plugs were lubricated with silicone grease and thoroughly rinsed with double-distilled water just before being placed into the ground glass joint. One plug was inserted while the solution was flowing and resulted in the filling line being loosened slightly to allow the solution to overflow the unplugged joint. The filling line was then removed and the second plug was immediately inserted. These plugs were held tightly in place by tension hooks (Scientific Glass Apparatus Co., Inc.) which did a better job of sealing the joints to prevent leakage than the usual glass hooks and springs. As soon as the cell was

plugged a sample of the solution was collected from the filling line for determination of the concentration. During some of the early runs samples were taken of the solution entering and leaving the cell and showed no difference in concentration.

The procedure described above was used for each run in the temperature range of 100 to 110°C, but at higher temperatures the ground glass joints would not hold the pressure. For these runs the cells were cleaned and filled in the usual manner, except no silicone grease was used, and the cells were permanently sealed by fusing the glass below the ground joints. Silicone grease was not used because when the glass was heated the grease decomposed and badly contaminated the solution before the glass could be sealed. These sealed cells were agitated for at least 18 hours after each run in order to redissolve the calcium sulfate which had precipitated. Agitation was provided by rotating the cells at 2 rpm on an axis perpendicular to the plane of the cells.

Just prior to a run the bath temperature was raised about 0.25-0.30°C above its control temperature by increasing the voltage to the manual heater and without changing the control point of the sensing element. This was done so the bath temperature would adjust rapidly to the control temperature when the conductivity cell was placed into the bath. While the temperature was being raised the filled conductivity cell was mounted above the bath, the side arms were filled with mercury, and the cell was connected to the bridge.

The run was started at time zero by turning on the chart drive of the recorder and immersing the cell into the bath. The bridge was maintained in approximate balance by adjusting R_4 and C_4 while the temperatures of the cell and the bath adjusted to the control temperature. During this transient period the voltage divider was set to zero so that no signal was sent to the recorder since the rapid adjustments of R_4 and C_4 would make recording of the bridge output voltage useless. When the resistance of the cell began to level off adjustments were made in the ground circuit and the voltage divider was set to 0.001. Tests with water filled cells showed that the cell temperature adjusted to within less than 1°C of the bath temperature in 3-4 minutes. Experience obtained from the experimental runs indicated that approximately 10-12 minutes were required before the temperature leveled off enough to cause negligible change in the cell resistance. When thermal equilibrium was obtained R_4 was adjusted to a value slightly below the balance value to avoid working in the "dead zone" of the amplifier and to prevent going through the null balance of the bridge and encountering the resulting phase change in the output voltage. Throughout all experimental runs C_1 was 476 picofarads and $R_1 = R_2 = 3{,}500$ ohms for runs 1-51 and $R_1 = R_2 = 5{,}000$ ohms for runs 52-76.

Once thermal equilibrium was established the recorded voltage would hold fairly steady until nucleation occurred at which time the recorded voltage would start to increase and would continue to do so as more calcium sulfate was precipitated from solution. The time at

which the voltage began to increase because of an increase in the cell resistance was called the nucleation time, τ . The Beckman differential thermometer could indicate temperature fluctuations as small as 0.001°C and it was observed during the run to be certain that changes in the recorded voltage were not caused by temperature fluctuations. The temperature of the bath, the values of R_4 and C_4 , and the Beckman reading were periodically recorded throughout the run. After the recorded voltage had increased 2 or 3 millivolts, R_4 was adjusted to a value slightly below its balance value to determine the sensitivity of the detector in millivolts per ohm change in R_4 . The run was terminated when the nuclei had grown to visible crystallites, whereupon the cell was removed from the bath and examined to be certain that the crystals had deposited on the steel specimen rather than elsewhere in the cell.

A photograph of a recording of the amplified and rectified output voltage of the bridge obtained with this procedure is reproduced in Figure 6. The straight line at the beginning of the run corresponds to the time when the voltage divider was set to zero and the three short lines showing a decreasing voltage represent an increasing temperature of the solution for three values of R_4 . The recorder had four input terminals and normally printed a + mark with a number beside it corresponding to the input terminal connected to the potentiometer circuit of the recorder. The switching mechanism was disengaged during this investigation and only the amplified bridge voltage was recorded regardless of the number being printed. Because of the slow chart speed the printing overlapped and resulted in two lines with the left one corresponding to the bridge voltage.

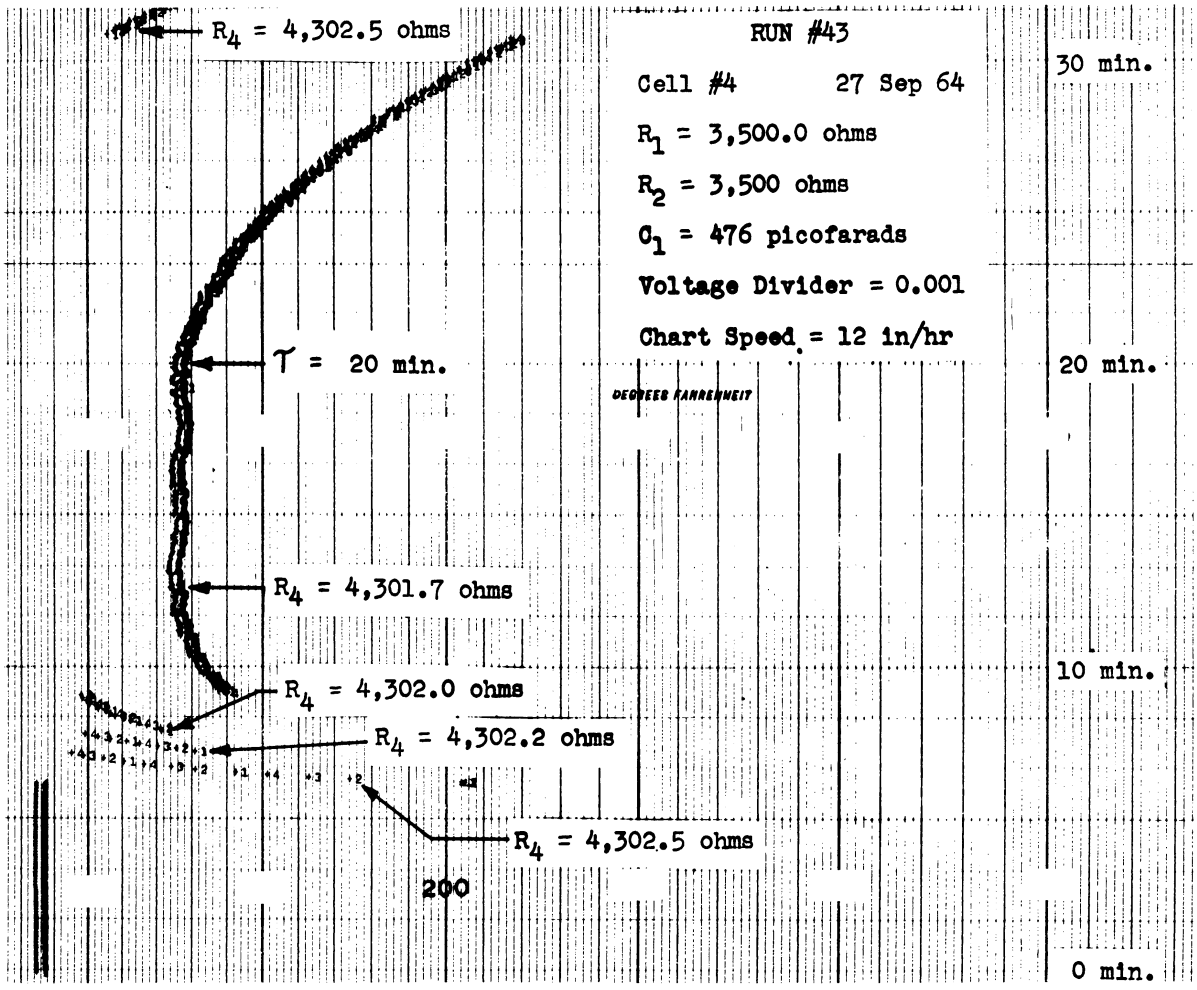

Figure 6. Photograph of Voltage Recording from Run No. 43.

4. Electron Microscopy

A different procedure was used to obtain samples for electron microscopic examination since the stainless steel samples with their deposit of calcium sulfate could not be removed from the conductivity cells in time to prevent substantial dissolution of the crystals. Glass test tubes and plugs were formed by sealing the unground end of the outer and inner parts, respectively, of ₹ 10/30 ground glass joints. Several of these tubes were filled with calcium sulfate solution, a stainless steel sample was placed in each tube, and the tubes were then sealed with silicone grease and placed in the constant temperature bath to achieve supersaturation. After a period of time each tube was removed from the bath, the sample was removed from the tube, and immediately rinsed with double-distilled water to remove adhering calcium sulfate solution and then with acetone to remove excess water so that the deposited crystals would not be redissolved. Two stage carbon-collodion replicas were then made of the surfaces of the stainless steel samples for examination in the electron microscope. In this replication technique the samples were coated with a thick solution of collodion, made by diluting USP collodion solution with an equal volume of amyl acetate, and 200 mesh electron microscope specimen grinds were embedded in the wet collodion which was allowed to dry slowly by evaporation of the solvent at room temperature. The dry collodion films with the embedded specimen grids were then stripped from the stainless steel sample with a pair of fine tweezers, placed in a vacuum evaporator, shadowed with a platinum-palladium alloy at a shadowing angle of about 45°, and then coated

with a layer of carbon by the evaporation of a 2 to 3 mm length of 1 mm diameter carbon rod placed about 10 cm vertically above the replica. The grids bearing the combined collodion-carbon replicas were then placed in covered petri dishes on several layers of filter paper saturated with amyl acetate and allowed to stand overnight to dissolve the collodion leaving the shadowing metal and the carbon replica on the grid. A very advantageous feature of this replication technique was that it behaved much like an extraction relication process[35] since many of the crystallites that had formed on the stainless steel were removed with the collodion film and were left embedded in the carbon replica when the collodion was dissolved. This made it possible to obtain electron diffraction patterns of the crystallites for identification of the hydrated form of calcium sulfate.

5. Experimental Uncertainties

The nucleation times were determined from the voltage recordings and the accuracy with which they could be determined depended on how rapidly the recorded voltage increased from the steady state value. For runs with nucleation times around 10 to 20 minutes the voltage increased rapidly after detectable nucleation had occurred and the time could be determined to less than 0.5 minute. For runs with nucleation times of the order of 100 minutes the voltage increased slower because of the slower rate of nucleation and the nucleation times could be determined only within about 2 minutes. A reasonable estimate of the average uncertainty in the nucleation times is $\pm$ 3%.

The accuracy of the solution concentrations depends on the sensitivity of the end point of the titration, on how well the versene concentration is known, and on the accuracy of the volumetric glassware. The end point of the titration was detectable within one drop of the versene solution and the reproducibility was usually within ± 0.03 ml of the versene solution. The versene was standardized by titrating pipetted samples of calcium chloride solutions whose concentration was known within ± 0.1%. The pipet volume was accurate to ± 0.1% and the buret accuracy was within ± 0.1%. Some of the inaccuracies of the buret and pipet were canceled out since the same pipet and buret were used to determine the concentration of the versene and the calcium sulfate solutions and a reasonable estimate of the accuracy of the calcium sulfate concentrations is ± 0.2%.

The cell resistance is equal to the value of R_4 since $R_1 = R_2$ during the experimental work. The accuracies of R_1, R_2, and R_4 are reported as ± 0.05% by the manufacturers and neglecting the effect of the small capacitances in the bridge arms introduces an error in the cell resistance of approximately 0.02%, as shown in Appendix E. The cell resistance may be assumed to have the same value as R_4 with an accuracy of ± 0.1%.

The bath temperatures were measured with calibrated mercury-in-glass thermometers having 0.1°C divisions. The calibrations of these thermometers is presented in Appendix B and the corrected temperatures are accurate to ± 0.03°C.

6. Experimental Difficulties

The two most troublesome problems encountered in this study were a result of the inverted solubility of calcium sulfate which made it necessary to heat the solutions to achieve supersaturation. One of the problems was leakage around the ground glass joints caused by pressure buildup as the cell was heated; the second was the unwanted nucleation that occasionally took place at the interface between the solution and the air pocket which was necessary to allow for thermal expansion of the solution. In addition, the range of nucleation times that could be determined was limited, and a minor problem was caused by the 3,000 cps harmonic signal produced by the bridge oscillator.

When the leakage around the ground glass joints was encountered it was generally very slow and resulted in loss of the water by evaporation rather than loss of the solution. This loss of solvent caused an increase in the concentration of the solution in the cell which resulted in a continual decrease of the cell resistance that made it impossible to determine the time at which the cell resistance began to increase as a result of nucleation.

Examination of the cells at the end of each experimental run indicated that the only other place nuclei formed, in addition to the metal surface, was at the air-solution interface. This interfacial nucleation probably was a result of dust particles in the air pocket that settled to the interface and it was noticed in about 10% of the runs. This undesirable nucleation had little or no effect on nucleation on the metal surface or its detection for two reasons: (1) the

nuclei which formed at the interface were retained there by surface tension and did not settle on the metal surface at the bottom of the cell; (2) these nuclei were formed approximately 6 inches above the metal sample and 3 inches above the electrodes so that they had virtually no effect on the concentration of the solution near the metal or between the electrodes. This latter reason was verified experimentally by runs which were terminated before nucleation had taken place on the metal surface but after nucleation had occurred at the air-solution interface and which had shown no detectable increase in the cell resistance.

The shortest nucleation times which could be detected by the above procedures was limited to about 10 minutes because of the time required for the cell to come to thermal equilibrium. For times shorter than this the resistance of the cell would still be changing because its temperature was still increasing making it impossible to tell when the cell resistance began to increase as a result of nucleation. Nucleation times longer than about 150 minutes were usually difficult to determine accurately because of variations in the bath temperature. The bath temperature could be maintained at $\pm$ 0.005°C or less for several hours but for runs with long nucleation times the nucleation rate was so slow that even these extremely small temperature fluctuations could overshadow the change in cell resistance caused by nucleation.

The small, stray capacitances that were not eliminated caused the bridge to be frequency sensitive so that when the bridge was balanced for one frequency it would be slightly unbalanced for other

frequencies. As a result, part of the 3,000 cps harmonic signal produced by the audio oscillator could not be completely balanced out making it impossible to obtain a complete null of the bridge output voltage. However, since the bridge was operated slightly unbalanced, as mentioned above, this 3,000 cps harmonic signal had no effect on the sensitivity for detecting resistance changes and did not present a serious problem.

VI. EXPERIMENTAL RESULTS

1. Results of Nucleation Studies

Nucleation times were measured for nominal solution concentrations of 1.0, 1.5, 1.8, 1.9, and 2.0 gms of $CaSO_4$ per 1000 gms of solution. The temperature of observation was varied over a range of less than 6.5°C for each concentration to determine the effect of the level of supersaturation on nucleation times. The numerical data tabulated in Appendix A show that the temperature ranges covered for each of the above concentrations were 128.1° to 130.7°C, 111.7° to 115.7°C, 104.2° to 110.0°C, 101.9° to 107.8°C, and 101.3° to 107.8°C, respectively.

The nucleation studies were first conducted using solution concentrations of 1.8, 1.9, and 2.0 gms of $CaSO_4$ per 1000 gms of solution. The results are shown in Figures 7-9 as plots of nucleation time versus X_c and X_T, based on Equations (26) and (27), with the straight lines determined by the method of least squares. There was no significant difference in the results from these three concentrations when plotted in the above manner so the results were pooled as shown in Figure 10. The investigation was then extended to concentrations of 1.0 and 1.5 gms of $CaSO_4$ per 1000 gms of solution using the permanently sealed cells described earlier. These concentrations produced the results shown in Figures 11 and 12 as plots of nucleation time versus X_c and X_T. A statistical analysis indicates that there is a significant difference in the lines for C = 1.0, 1.5, and 1.8 to 2.0 gms of

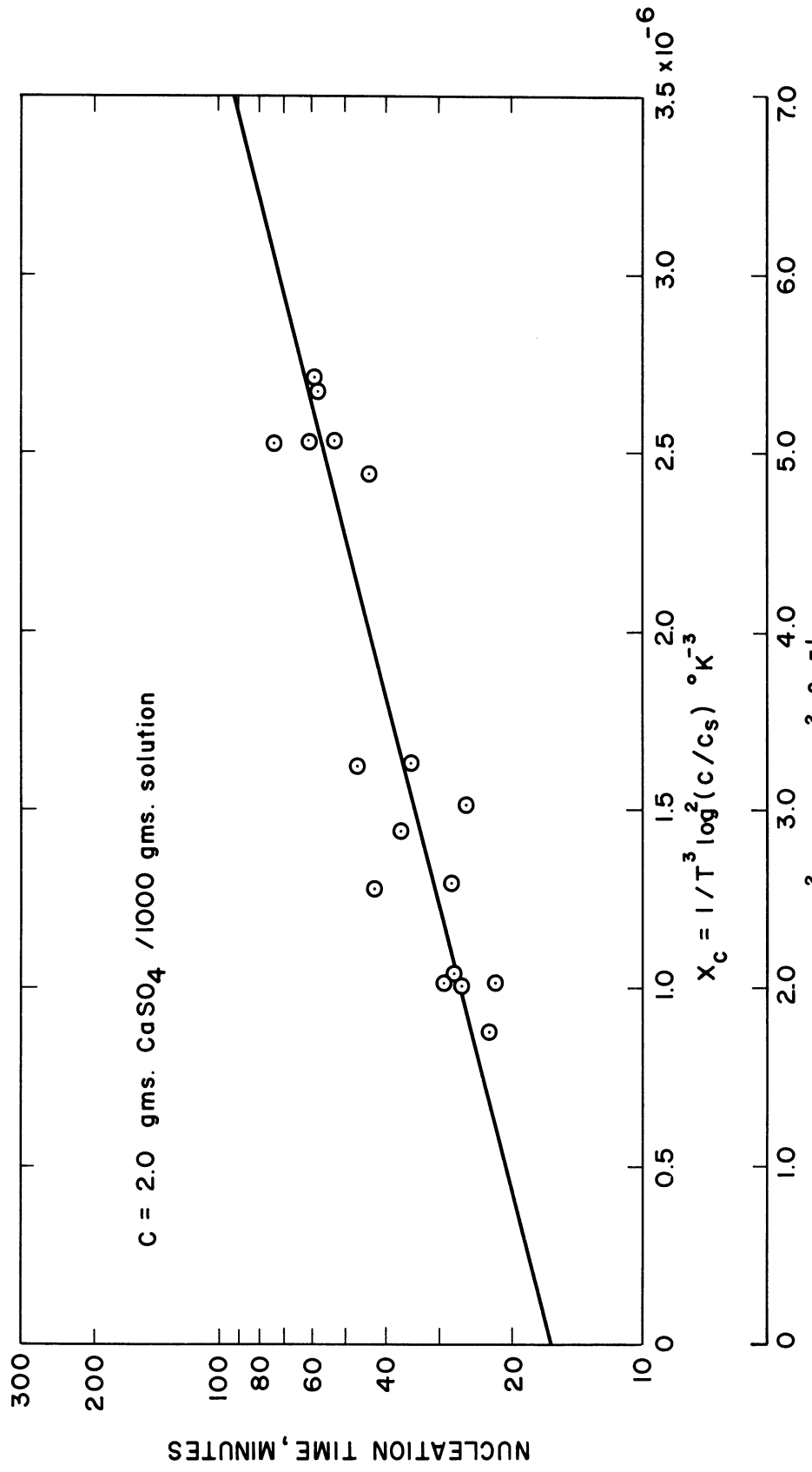

Figure 7. Log τ versus X_c and X_T for C = 2.0.

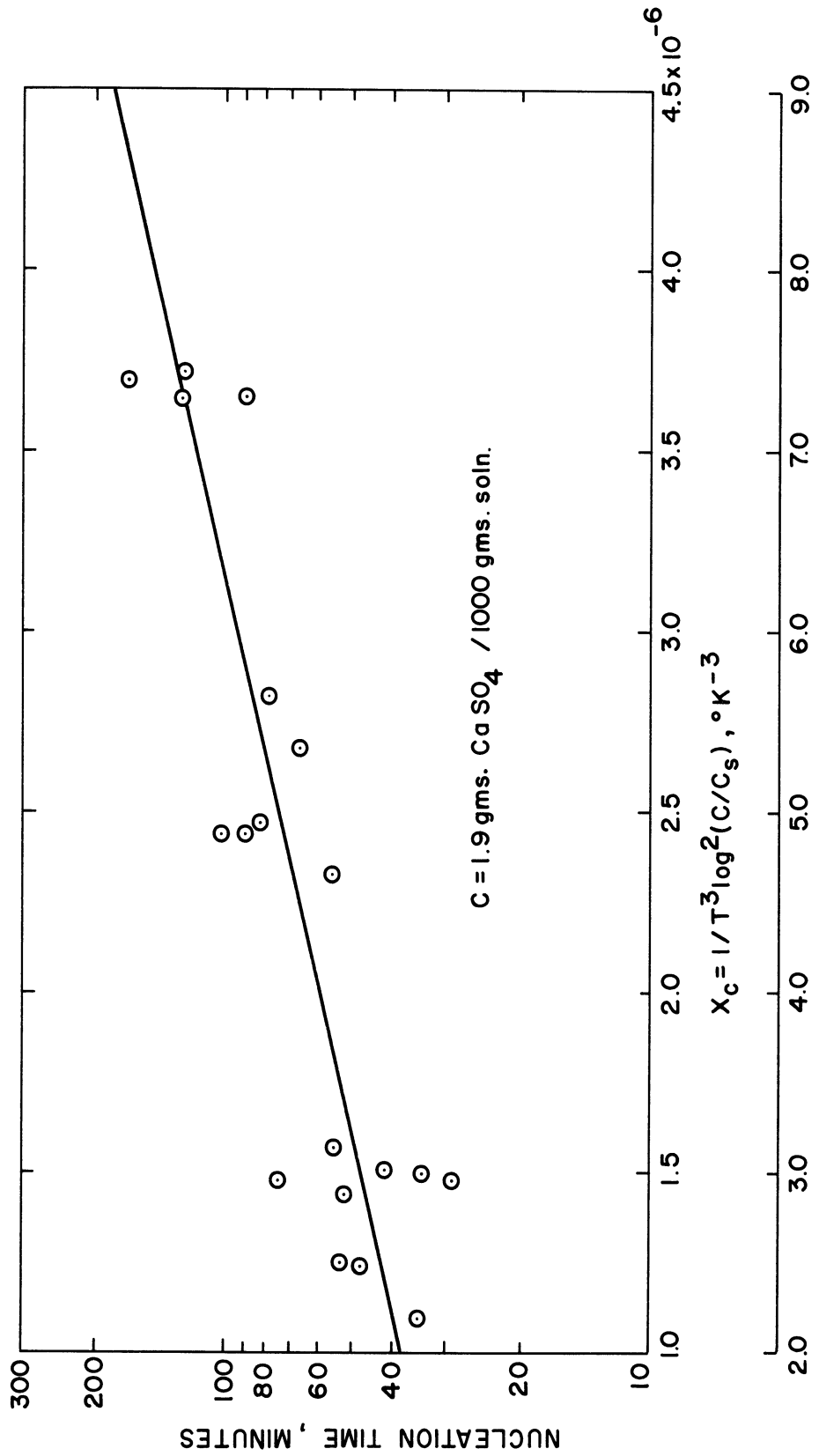

Figure 8. Log τ versus X_C and X_T for C = 1.9.

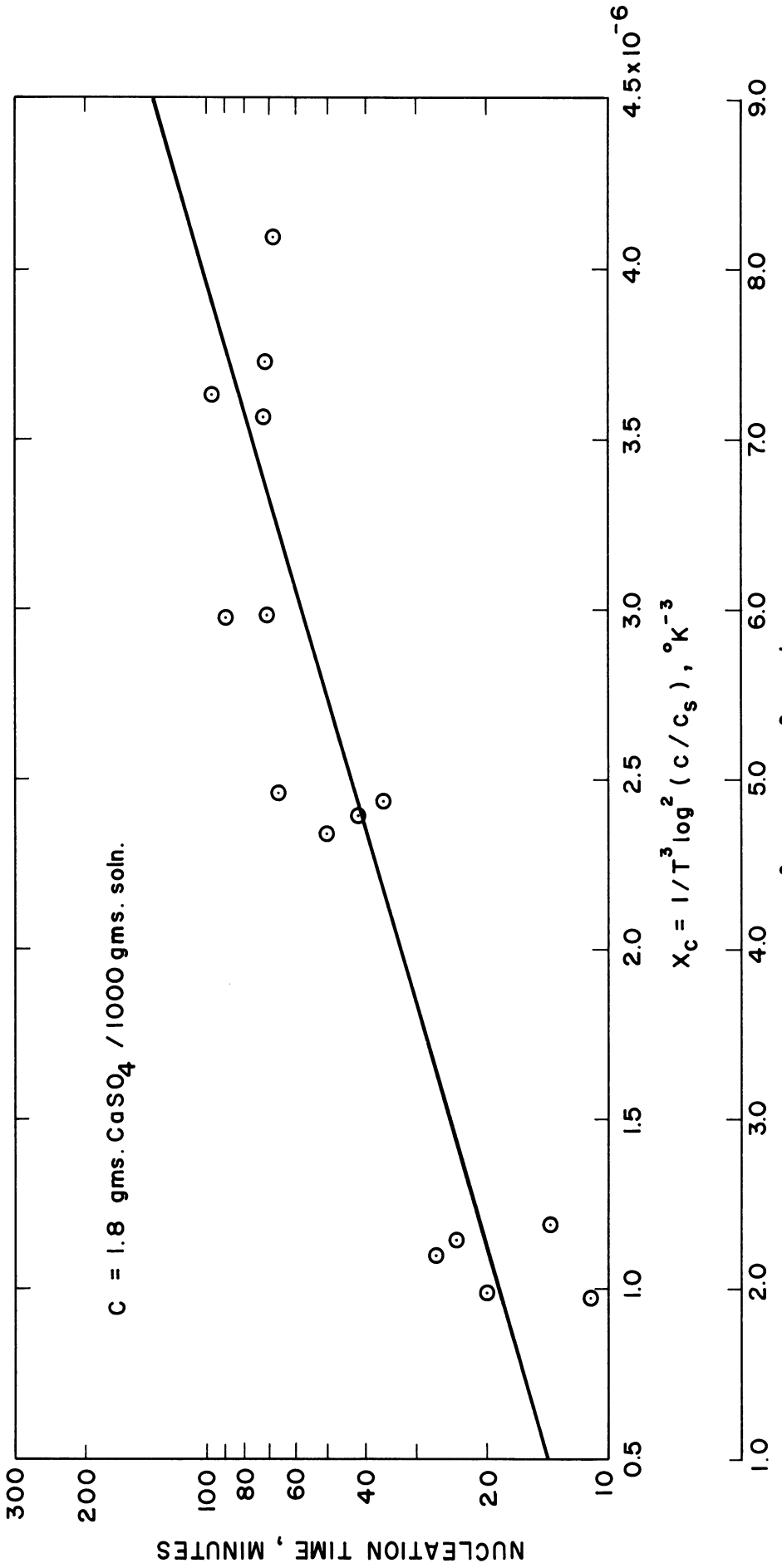

Figure 9. Log τ versus X_c and X_T for C = 1.8.

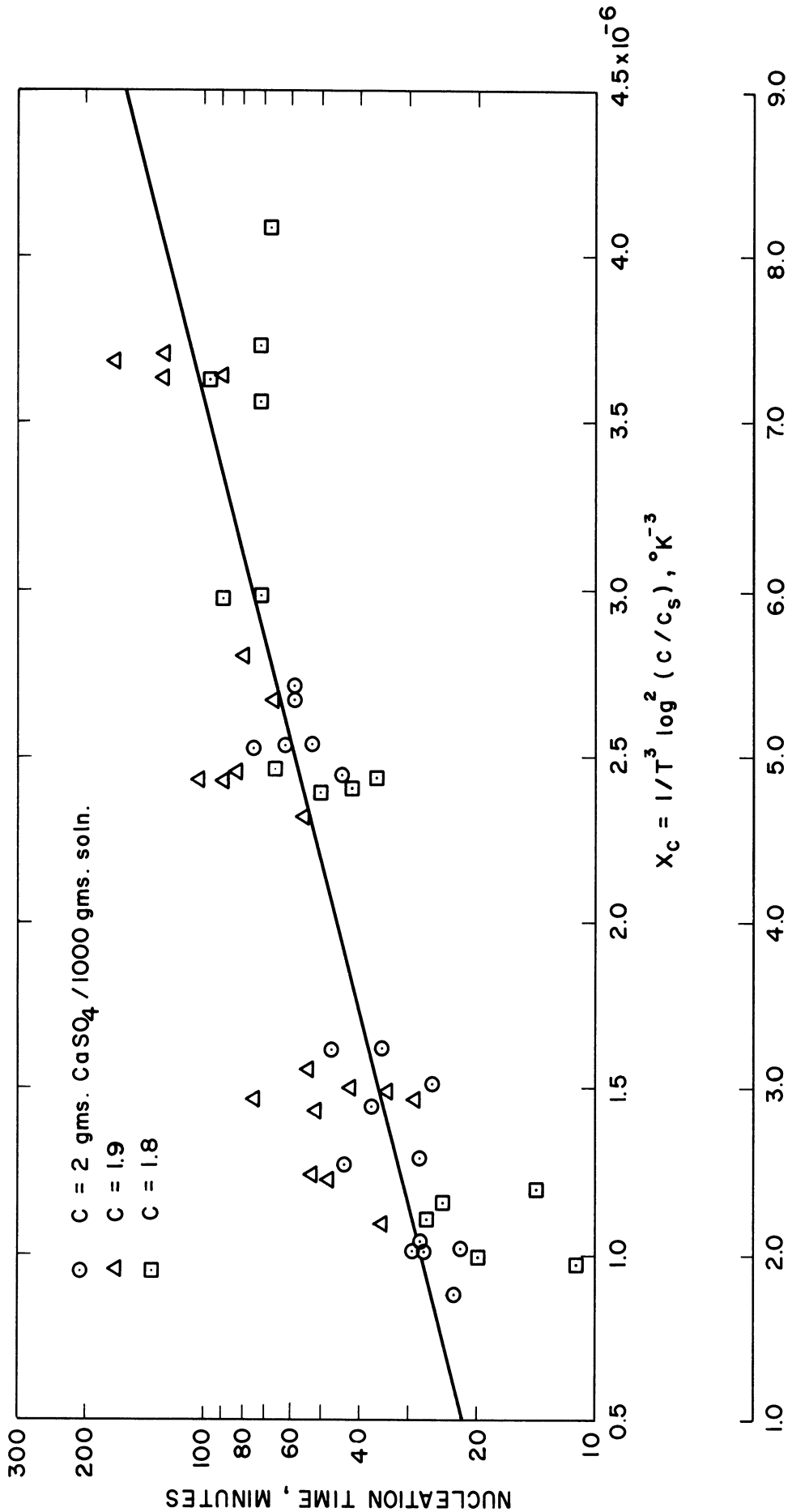

Figure 10. Log τ versus X_c and X_T for C = 1.8 to 2.0.

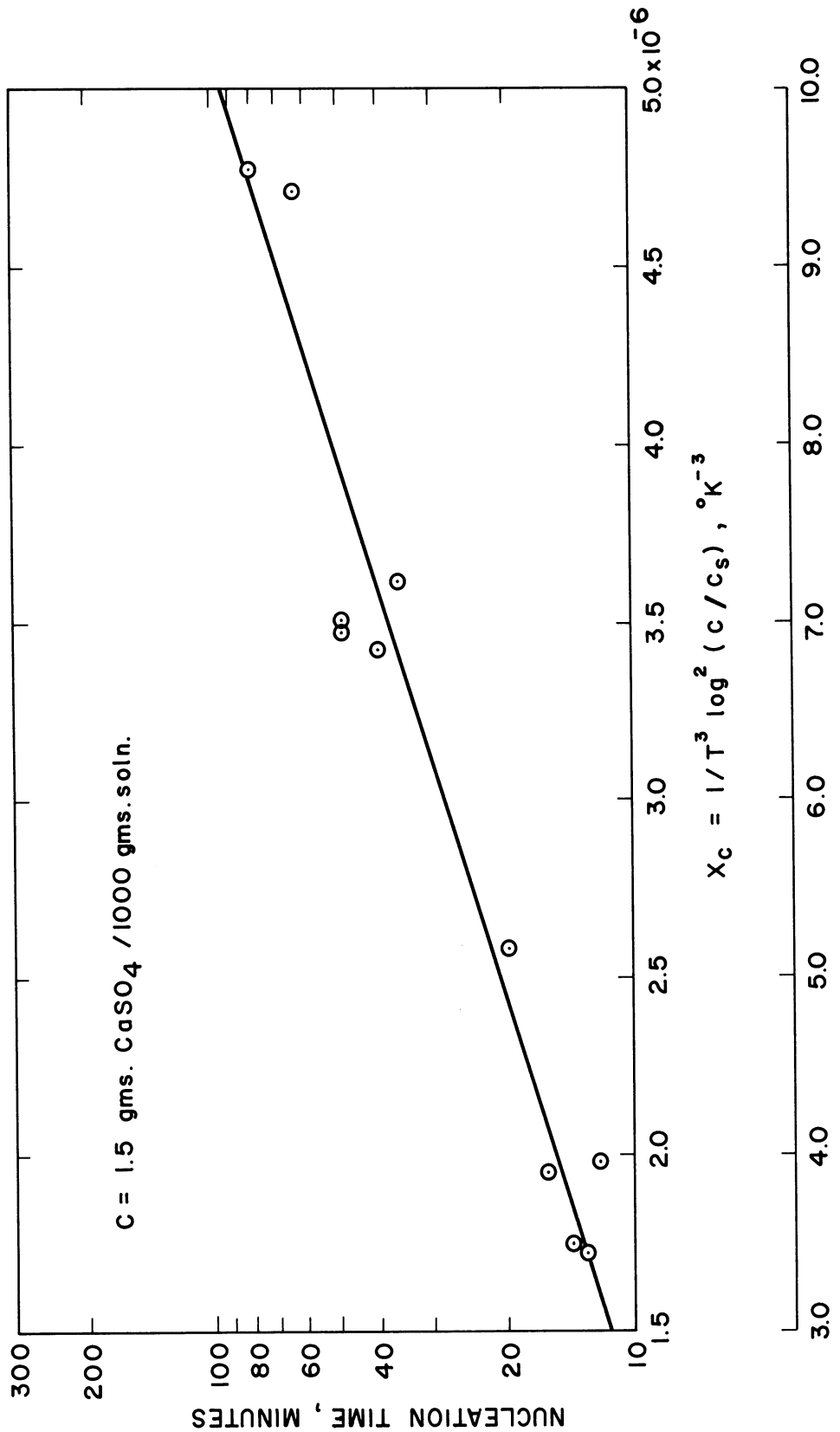

Figure 11. Log τ versus X_c and X_T for C = 1.5.

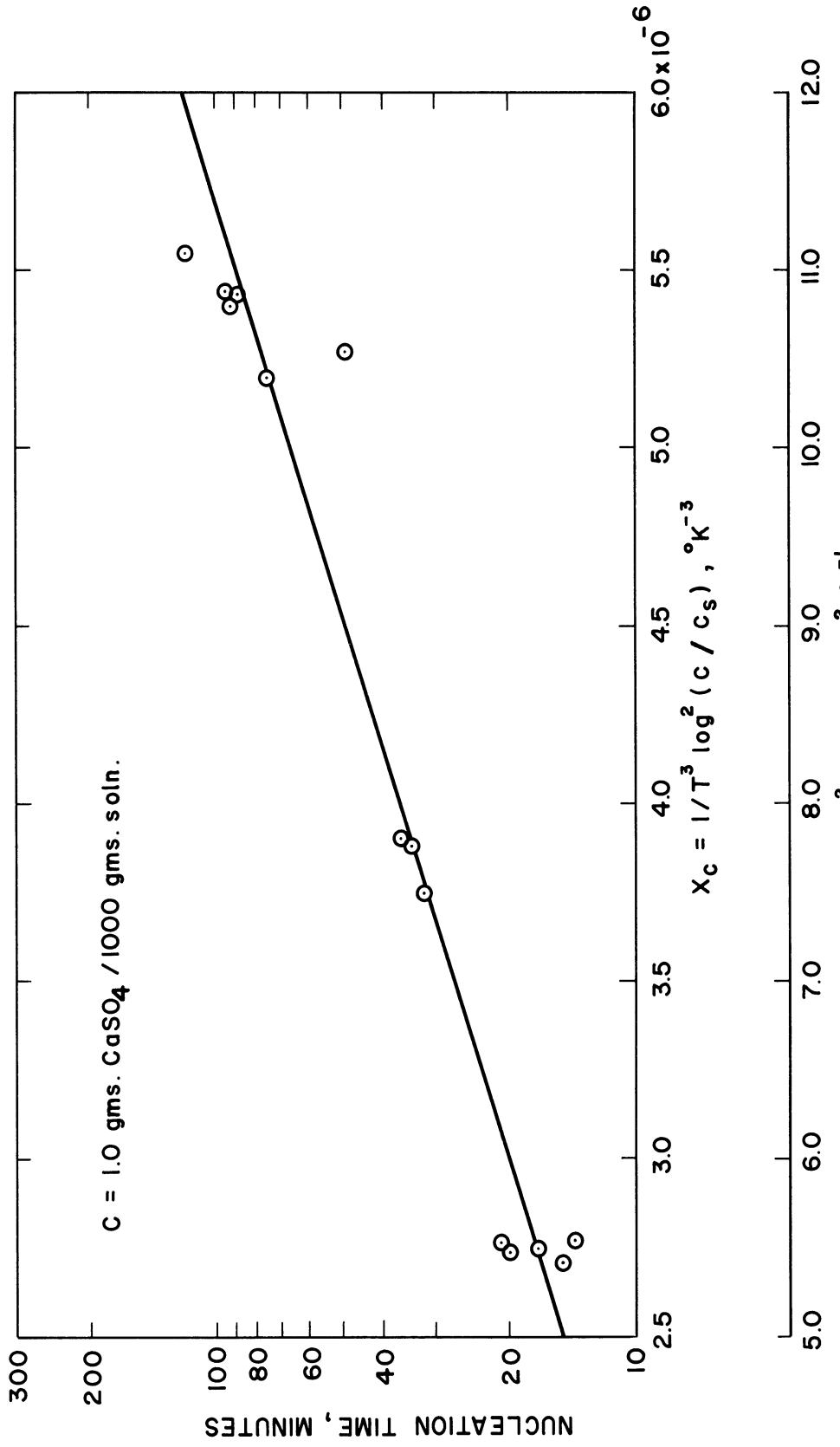

Figure 12. Log τ versus X_c and X_T for C = 1.0.

$CaSO_4$ per 1000 gms of solution. The lines from Figures 7-12 are plotted without the data points in Figure 13 to show their relation to each other and the slopes of these lines are listed along with their statistical 95% confidence limits in Table I.

TABLE I

SLOPES OF LOG τ VERSUS X_c AND X_T

Concentration (gms./1000 gms. solution)	Slope of Log τ versus X_c ($°K^3$)	Slope of Log τ versus X_T ($°K$)
2.00	$(2.15 \pm 0.59) \times 10^5$	0.107 ± 0.030
1.90	$(1.93 \pm 0.60) \times 10^5$	0.096 ± 0.030
1.80	$(2.44 \pm 0.73) \times 10^5$	0.122 ± 0.036
1.50	$(2.60 \pm 0.49) \times 10^5$	0.130 ± 0.024
1.04	$(2.61 \pm 0.41) \times 10^5$	0.130 ± 0.020
1.8-2.0	$(2.15 \pm 0.44) \times 10^5$	0.107 ± 0.022

The data presented in Figures 7-12 show that plots of log τ versus X_c and X_T for the experimental conditions used in this study yield straight lines as predicted by Equations (26) and (27). Comparison of the lines of Figure 13 indicates that the intercepts of these plots decrease with decreasing concentration and that the slopes are essentially independent of concentration. The decrease in the intercepts can be explained by the theoretical equations. The intercept of a semi-log plot of nucleation time versus X_c or X_T is K', which is inversely proportional to K by definition. According to Equation (15), K is approximately proportional to $T^{1/2}\exp(-\Delta F_D/kT)$

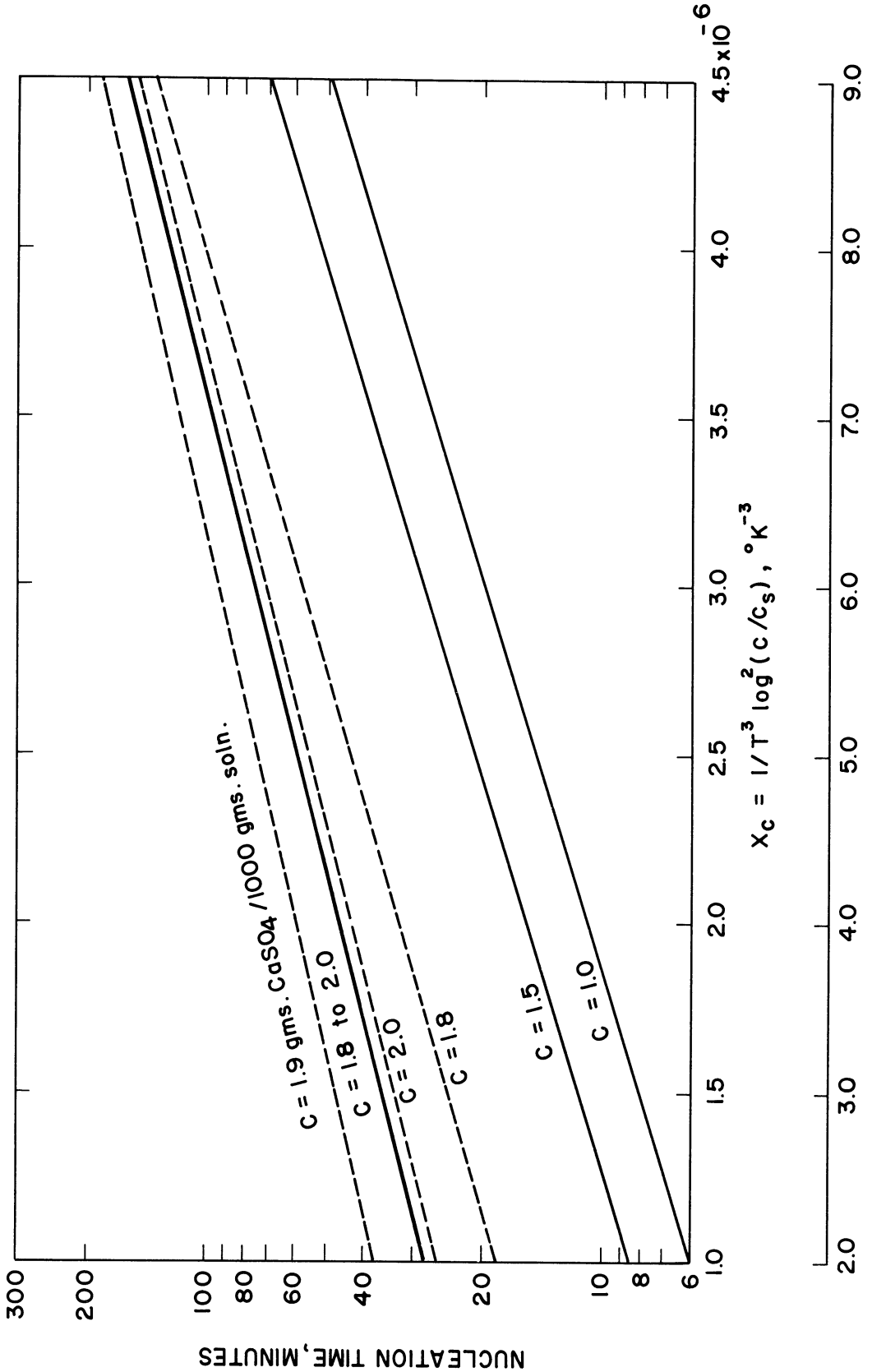

Figure 13. Comparison of Lines from Figures 7-12.

and will increase with an increase in temperature. As the concentrations of the calcium sulfate solutions are decreased it is necessary to increase the operating temperature to achieve the same value of X_c or X_T which in turn increases K and decreases K' . The definitions of the slopes in Equations (28) and (29) indicate that the slopes should change very little with decreasing concentration and the resulting higher temperature since most of the terms in these definitions are constants or change very little with temperature.

The scatter of the nucleation times is greater than their experimental uncertainty and may be attributed partially to lack of complete reproducibility of experimental conditions and partially to the random nature of the nucleation process. The effects of experimental reproducibility are readily seen by comparing the plots and confidence limits of the slopes for C = 1.8, 1.9 and 2.0 to those for C = 1.0 and 1.5 gms of $CaSO_4$ per 1000 gms of solution. The latter two concentrations were studied using sealed cells repeatedly while the other three concentrations were studied using a freshly cleaned and filled cell with a new stainless steel sample for each run. Some of the scatter for the three highest concentrations may be attributed to the slight difference in the concentrations from one run to the next as shown in Table A-1 in Appendix A. It is also possible that the surface area and surface condition of the metal might have varied from one run to another. The random nature of the nucleation process has long caused variability in the results of nucleation studies and others have also found scatter in the results obtained from the repeated nucleation of

sealed cells.[37,67] At any rate, the scatter obtained in this study is not any worse than that obtained by previous investigators.[2,59]

Although X_c and X_T have a theoretical basis, plots of the nucleation results using coordinates of temperature and concentration are of more practical use since they readily show the effects of temperature and concentration on nucleation times. Figures 14 and 15 are two such plots and they were obtained from the three solid lines in Figure 13. Nucleation time is plotted versus the degrees of superheating in Figure 14 with concentration as a parameter and shows the decrease in nucleation times for a given degree of superheating as the concentration is decreased. Conversely, it shows that for a given nucleation time the degrees of superheating must be decreased as the solution concentration is decreased. In Figure 15 concentration is plotted versus temperature with nucleation time as a parameter. The solubility curve used to analyze the nucleation data is also plotted in Figure 15 and, as indicated, it should theoretically correspond to an infinite nucleation time. The lines of constant nucleation time are roughly parallel to the solubility curve and indicate why some people accept the supersolubility concept. Of more practical importance, however, is the strong effect that temperature and concentration have on the nucleation time. It can be seen from Figure 15 that only a small change in concentration or temperature is required to change the nucleation time from 50 to 200 minutes. This effect becomes more noticeable as the temperature is increased. As a practical application of these results, an evaporator might be operated such that the residence time of the solution being

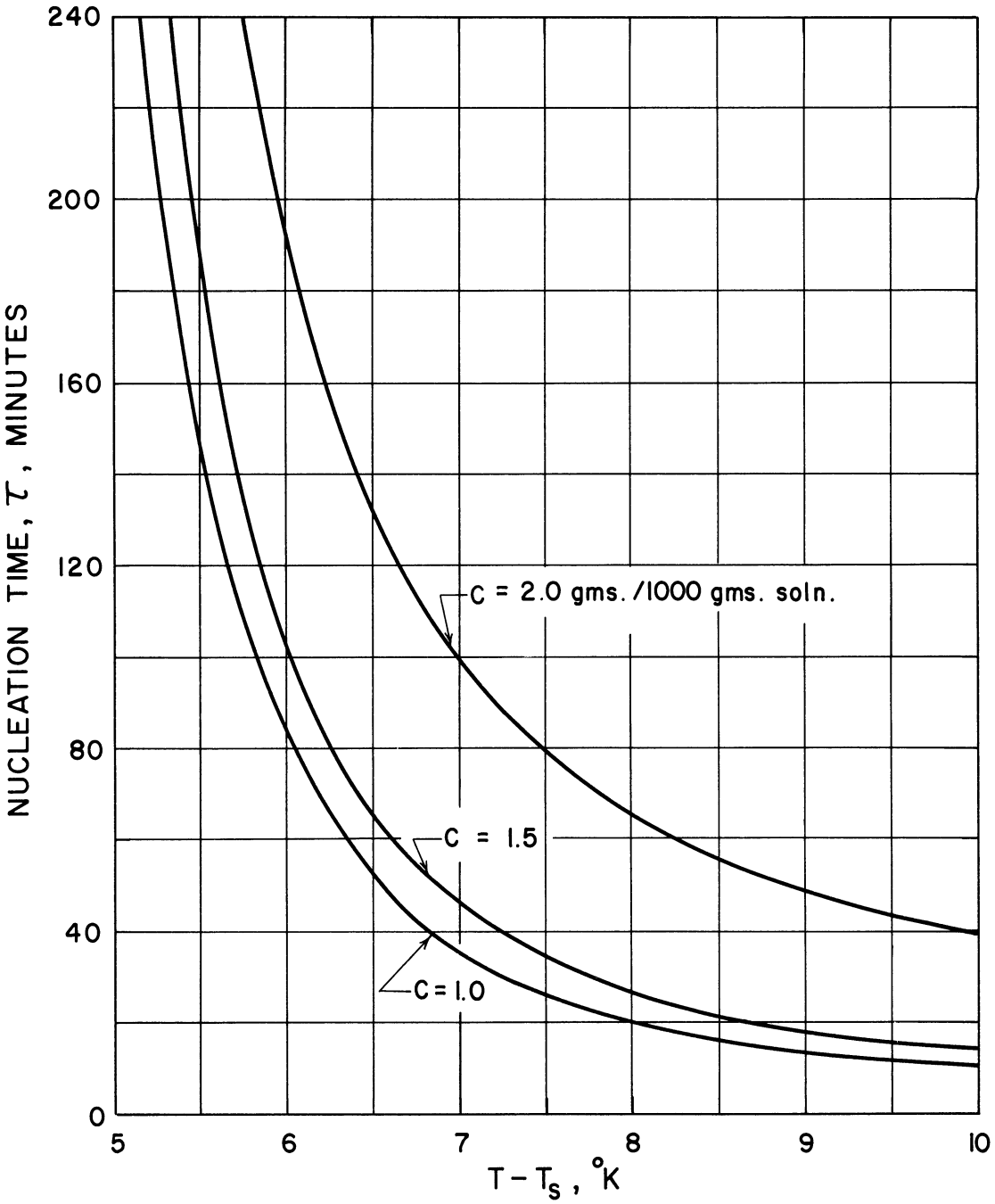

Figure 14. Nucleation Time versus Degrees of Superheating with Concentration as a Parameter.

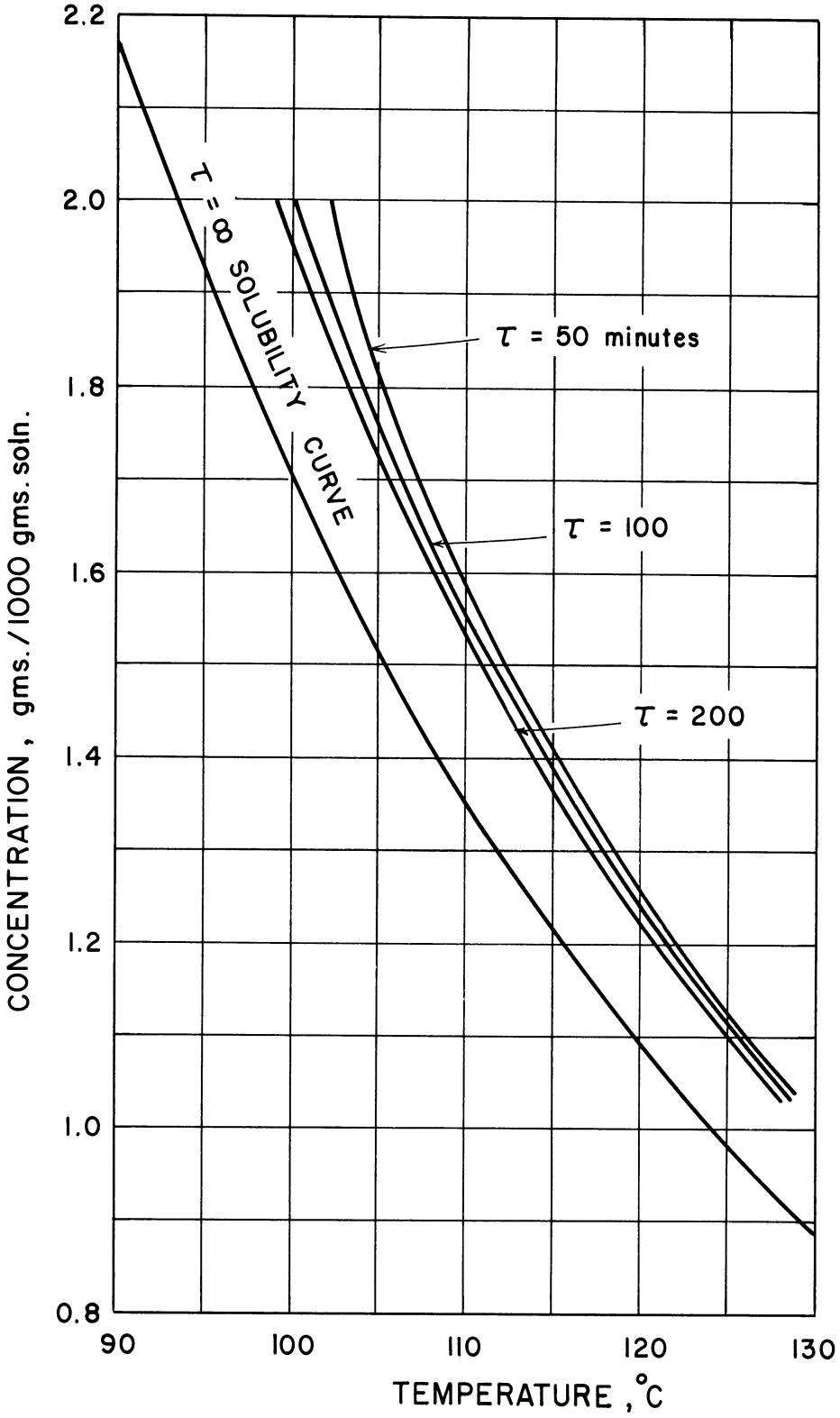

Figure 15. Concentration versus Temperature with Nucleation Time as a Parameter.

evaporated would be less than the nucleation time for the particular temperature and concentration being employed. It is apparent, however, that such an operation would require close control of the solution concentration and the evaporator temperature.

2. Determination of Calcium Sulfate Solubility

Solubility information on calcium sulfate is necessary to analyze the experimental data by the theoretical equations developed earlier. A search of the literature produced the solubility data for calcium sulfate hemihydrate shown graphically in Figure 16. An equation of the form

$$\log C = B_o + \frac{B_1}{T} + \frac{B_2}{T^2} \tag{41}$$

is useful in correlating solubility data[51] and was fitted to the literature data by a multiple regression analysis subroutine available on the IBM 7090 computer at the University of Michigan Computing Center. The constant B_2 was found to be insignificant yielding an equation with determined constants

$$\log C = -3.7508 + 1{,}481.2/T \tag{42}$$

where C is the concentration in gms of $CaSO_4$ per 1000 gms of solution and T is the absolute temperature in °K. This equation is shown graphically as the dotted line in Figure 16, and the dashed lines represent the statistical 95% confidence limits of the data. These limits show that there is extensive scatter of the literature data and if these limits are used to determine the uncertainties in X_T and X_C

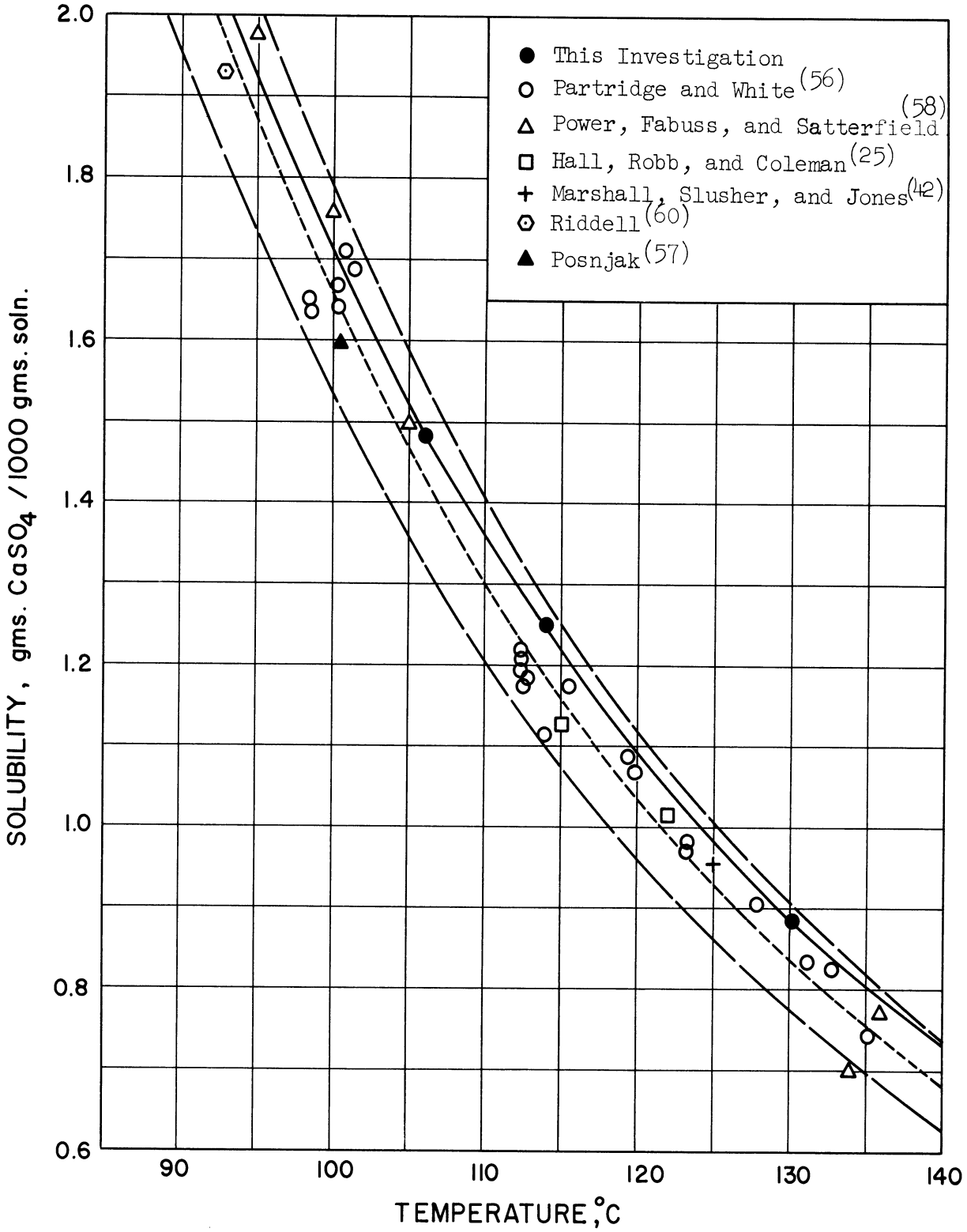

Figure 16. Experimental and Literature Data on the Solubility of Calcium Sulfate Hemihydrate in Water.

the range of variation is so large that the nucleation data cannot be reasonably interpreted. For example, a solution with a concentration of 1.8 gms/1000 gms. of solution supersaturated at 106°C would have $C_s = 1.43 \pm 0.11$ and $T_s = 96.5 \pm 3.2$°C from Figure 16. Calculations with these values give a range on X_c from 1.01×10^{-6} to 2.05×10^{-6} ($°K^{-3}$) and X_T from 2.20 to 9.24 ($°K^{-1}$) which nearly cover the ranges used in Figures 7-12. In order to hold the uncertainties in X_c and X_T to reasonable values, the solubility of calcium sulfate was determined for conditions and solutions similar to those used in the determination of the nucleation times.

Calcium sulfate solubility was determined at 106.0, 114.1, and 130.2°C by following the change in the electrical conductivity as the solute precipitated in a conductivity cell from an unstirred supersaturated solution. The equilibrium value of the conductivity was then used to determine the equilibrium concentration from a knowledge of the relationship between conductivity and concentration. The results of these determinations are shown in Figure 16. The solid line is given by

$$\log C = -3.5620 + \frac{1,414.9}{T} \qquad (43)$$

where C and T are as defined earlier, and is the solubility curve which was used to determine C_s and T_s for the calculation of X_c and X_T. The confidence interval for C_s is $\pm 0.5\%$ and for T_s is ± 0.03°C.

The concentration, conductivity, and resistance of the solution are related by the expression

$$\Lambda R_c C' = 1000 k_c \qquad (44)$$

where Λ is the equivalent conductivity in cm^2/ohm, R_c is the resistance of the solution in the cell in ohms, C' is the concentration of the solute in equiv./liter of solution, 1000 is a conversion factor with the units $cm^3/liter$, and k_c is a cell constant which depends only on the geometry of the cell and has the units cm^{-1}. The constants of the cells used in this study were determined by measuring the resistance of the cells at 100.00 ± 0.02°C when they were filled with a sodium chloride solution with a concentration of 0.01207 equiv./liter measured at 25°C. At 100°C this solution has a concentration of 0.01160 equiv./liter and an equivalent conductivity of 333.2 cm^2/ohm as interpolated from the International Critical Tables.[32] The values of the cell constants determined by these measurements are presented in Table II and are good to ± 0.2%. These cell constants were used in calculating the equivalent conductivity for each nucleation run presented in Table A-1.

TABLE II

CELL CONSTANTS

Cell	R_c (ohms)	k_c (cm^{-1})
2	3,891	15.04
3	4,750	18.36
4	4,797	18.54
5	5,048	19.51
6	4,530	17.51
7	4,706	18.19

Five of these cells were cleaned, filled, and permanently sealed as described in the section entitled Experimental Procedures and were used to determine the conductivity of calcium sulfate as a function of concentration at 106.0, 114.1, and 130.2°C. The results of these determinations are tabulated in Table III and are presented graphically in Figure 17 along with data obtained from the International Critical Tables. The point at 100°C agrees very well with the data from ICT and was obtained by a linear extrapolation of a plot of Λ versus temperature from the data in Table A-1 for a concentration of approximately 2.0 gms./1000 gms. of solution.

TABLE III

RESULTS OF CONDUCTIVITY MEASUREMENTS

Cell	T °C	C gms./1000 gms.	C' equiv./liter	R ohms	Λ cm^2/ohm
4	106.0	1.788	0.02506	4,443	166.5
5	106.0	1.497	0.02098	5,338	174.2
3	106.0	1.237	0.01733	5,766	183.7
7	106.0	1.039	0.01456	6,465	193.4
5	114.1	1.497	0.02084	5,276	177.4
3	114.1	1.237	0.01722	5,682	187.6
7	114.1	1.039	0.01447	6,365	197.5
7	130.2	1.039	0.01426	6,385	199.8
6	130.2	0.796	0.01093	7,396	216.6

Solubility determinations were carried out at 114.1 and 130.2°C by placing a sealed cell in the bath at a temperature which would cause the solution to become supersaturated, and maintaining this temperature

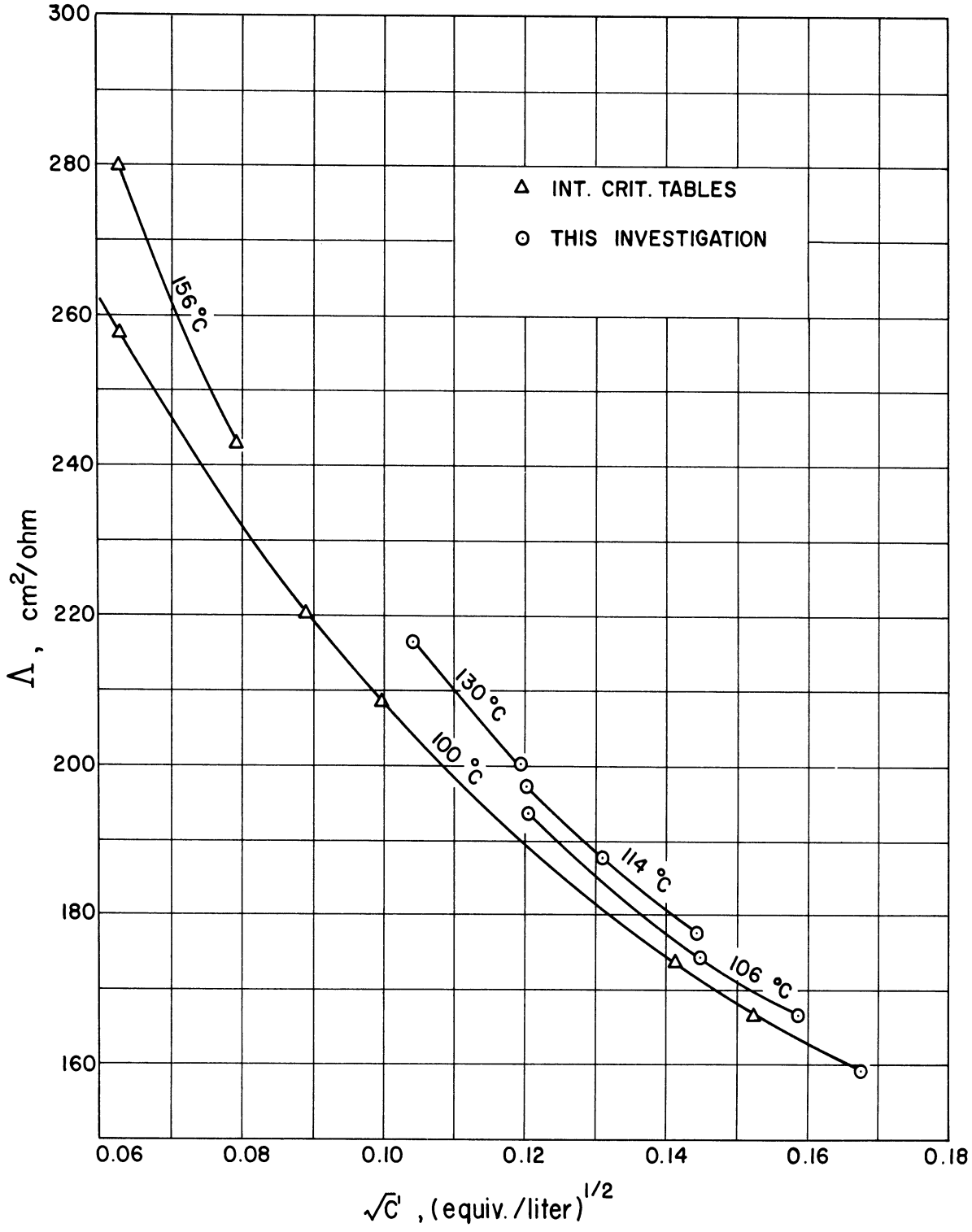

Figure 17. Equivalent Conductivity of Calcium Sulfate.

until the resistance of the cell became steady, indicating that precipitation of calcium sulfate had stopped and that saturation had been reached. The bath temperature was then raised 2-3°C for 3-4 hours to cause further precipitation and then returned to the original temperature resulting in the solution being unsaturated. Some of the precipitated calcium sulfate would redissolve until saturation was reached as evidenced by no further change in the cell resistance. This technique verified the attainment of equilibrium since saturation was approached from two directions. The procedure used to determine the solubility at 106.0°C was similar except that saturation was achieved only by precipitation and not by redissolving some of the precipitate. The temperatures were maintained within $\pm$ 0.02°C throughout the runs.

The results of these solubility determinations were presented graphically in Figure 16 and are tabulated in Table IV. The concentration C was obtained from a plot of $\Lambda C'$ versus C which is nearly linear and eliminates the trial and error involved in using a plot of Λ versus C . Equation (44) may be used to calculate $\Lambda C'$ directly knowing the cell constant and resistance. The saturated concentrations determined from the two approaches to equilibirum differ only slightly and the saturated concentration was taken as the average of the two values. Equation (43) was obtained by a linear regression of the solubility data presented in Table IV.

TABLE IV

RESULTS OF SOLUBILITY DETERMINATIONS

Temp. (°C)	Time at Temp. (hrs.)	Final Resistance (ohms)	Direction of Approach	Cell No.	C (gms. $CaSO_4$/ 1000 gms.soln.)
106.0	126	5,106	Precipitation	4	1.481
114.1	140	5,970	Precipitation	5	1.256
114.1	32	6,016	Dissolution	5	1.244
130.2	96	7,122	Precipitation	7	0.889
130.2	41	7,156	Dissolution	7	0.881

3. Results of Electron Microscopy

Examples of the electron micrographs and the electron diffraction patterns obtained from the electron microscopic examination of the stainless steel samples are shown in Figures 18-20. The crystallites in Figures 18 and 19 were deposited from a solution with a concentration of 2.0 gms $CaSO_4$ per 1000 gms of solution after being heated for 10 and 20 minutes, respectively, at 111.6°C. As shown by these figures, the crystallites were needle-like, had no particular orientation on the surface of the metal, and appeared to be uniformly distributed over the surface. The crystallites in Figure 18 are approximately 500 Å wide and 1,500 Å long while those in Figure 19 are approximately 1,000 Å wide and 10,000 Å long. This increase in the ratio of length to width as the crystals develop means that the rate of growth in the length direction was faster than the rate of growth in the width direction.

Figure 18. Calcium Sulfate Deposited after 10 Minutes at 111.6°C, C = 2.0, x 43,000.

Figure 19. Calcium Sulfate Deposited after 20 Minutes at 111.6°C, C = 2.0, x 43,000.

The d values determined from selected area diffraction patterns like the one in Figure 20 were compared with standard d values reported for calcium sulfate hemihydrate as presented in Table V.

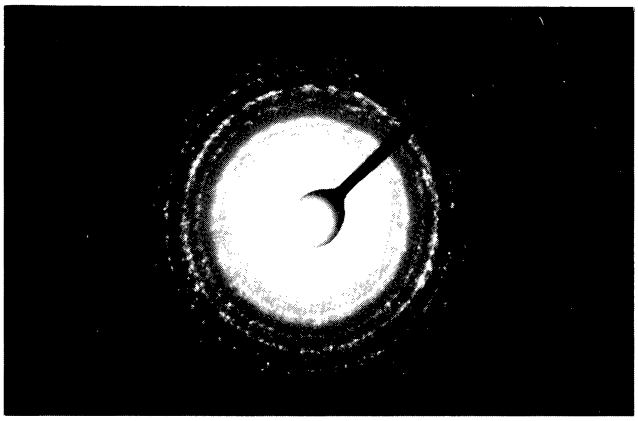

Figure 20. Electron Diffraction Pattern of Calcium Sulfate Deposit.

TABLE V

COMPARISON OF ELECTRON DIFFRACTION DATA FROM CALCIUM SULFATE DEPOSITED ON STAINLESS STEEL WITH DATA REPORTED FOR $CaSO_4 \cdot 1/2\ H_2O$

Electron Data*		$CaSO_4 \cdot 1/2\ H_2O$*	
d(Å)	I	d(Å)	I
5.93	M	5.98	S
		4.35	W
3.46	M	3.45	M
2.97	S	2.98	S
2.81	S	2.78	S
2.70	W	2.69	W
2.37	M	2.33	W
		2.26	W
		2.20	W
2.13	M	2.12	M
2.00	W	1.99	W
		1.89	M
1.84	M	1.84	S
		1.72	W
1.69	M	1.69	M

* I = relative intensity: S = strong, M = medium, W = weak

The agreement between the d values is as good as can be expected and indicates that calcium sulfate hemihydrate is the form which was deposited during the nucleation studies. This was also verified by the solubility studies described above since the solubilities were determined for experimental conditions similar to the ones used for the nucleation studies and the results fell within the range of data reported in the literature for the solubility of calcium sulfate hemihydrate.

4. Calculated Values of Activation Energy, Interfacial Energy, and Size of the Nuclei

The slopes of the straight lines obtained by plotting $\log \tau$ versus X_C and X_T may be used to calculate the activation energy for nucleation, the crystal-solution interfacial energy, the size of the nuclei, and the number of molecules in the nuclei. The activation energy may be calculated directly from the slopes given in Table I using Equations (34) and (35). However, calculation of the number of molecules in the nuclei requires a value for the heterogeneous nucleation factor, f, while calculations of the crystal-solution interfacial energy and the size of the nuclei requires information on the shape factor, S^j, as well as f.

A reasonable value for the shape factor can be calculated by assuming the nuclei to be hexagonal since this is the shape of the unit cell.[8,18,55] First consider the case where the nucleus forms homogeneously and let h^1_{i*} and h^2_{i*} be the perpendicular distances from the center of the nucleus to the lateral faces and the bases,

respectively. It will be assumed that the interfacial energies are the same for all faces since they cannot be determined individually from the results of this investigation. It follows from Equation (3) that $h^1_{i*} = h^2_{i*} = h_{i*}$ and the nucleus will have a hexagonal base with a radius of h_{i*} for the inscribed circle, a height of $2h_{i*}$, and a volume of $12(h_{i*})^3 \tan 30°$. When a nucleus forms heterogeneously on a surface the interfacial energy of the face in contact with this surface will be decreased and, as shown by Equation (3), this face will be closer to the center of the nucleus than it would be if the heterogeneous surface was not present. This will result in a decrease of the volume of the nucleus from that just calculated for the homogeneous case. Since the ratio of the heterogeneous volume to the homogeneous volume is f, the volume of the nucleus formed heterogeneously is $V_i = 12f(h_{i*})^3 \tan 30°$ and combining this with Equation (5) yields $S^j = 20.78f \cong 21f$. This value for S^j is based on a nucleus whose length and width are the same but the electron micrographs in Figures 18 and 19 show the length of the crystallites to be greater than the width. It was pointed out, however, that the ratio of the length to width increased as the crystallites grew so that it is quite possible that the nuclei, which are much smaller than the crystallites shown in these micrographs, have a ratio of length to width near unity.

Calculation of the heterogeneous nucleation factor, f, is nearly impossible since it requires a knowledge of the crystal-solution, crystal-steel, and steel-solution interfacial energies as well as the

orientation of the nucleus on the stainless steel surface. Values can be calculated for i^*f, $h_{i^*}f^{2/3}$, and $\sigma f^{2/3}$ from the experimental data without knowing f using Equations (30) to (33), (36) to (37), and the shape factor determined above.

Calculated values of the activation energy (A) and the modified forms of the interfacial energy ($\sigma f^{2/3}$), size of the nucleus ($h_{i^*}f^{2/3}$), and the number of molecules in the nucleus (i^*f) are presented in Tables VI and VII where the confidence intervals are determined from the confidence intervals for the slopes given in Table I. The solid lines in Figure 13 were used to calculate the values in Table VII and C was taken as 2.0 for the pooled data to calculate the value of T for a given value of X_c and X_T. A value of 52.8 cm^3/mole was used for the molal volume of calcium sulfate hemihydrate.[55] The differential heat of solution, determined from a plot of log C versus 1/T,[12,82] was found to be constant at -12,950 cal/mole. According to Equation (39), $m_c = (Q/2.303R\nu)^2 m_T = (1,414)^2 m_T = (2.0 \times 10^6) m_T$ as it does in Table I. It was also shown in the development of the theoretical equations that the calculated values for the activation energy, the interfacial energy, the number of

TABLE VI

CALCULATED VALUES OF $\sigma f^{2/3}$

C gms./1000 gms. soln.	$\sigma f^{2/3}$ (ergs/cm^2) From Log τ versus X_c	From Log τ versus X_T
1.8 - 2.0	5.05 ± 0.35	5.05 ± 0.35
1.5	5.38 ± 0.33	5.38 ± 0.33
1.0	5.39 ± 0.28	5.38 ± 0.28

TABLE VII

CALCULATED VALUES OF A, i*f, AND $h_{i*}f^{2/3}$

X_c	X_T	T	From log τ versus X_c			From log τ versus X_T		
			A	i*f	$h_{i*}f^{2/3}$	A	i*f	$h_{i*}f^{2/3}$
$°K^{-3}$	$°K^{-1}$	°K	kcal/mole		Å	kcal/mole		Å
			C = 2.0 gms./1000 gms.soln.					
$2.0x10^{-6}$	4.0	375.9	0.74±0.15	4.4±0.9	3.82±0.26	0.74±0.15	4.4±0.9	3.82±0.26
4.0	8.0	373.1	1.47±0.30	12.4±2.5	5.38±0.37	1.46±0.30	12.3±2.5	5.37±0.37
6.0	12.0	371.9	2.20±0.45	22.6±4.6	6.58±0.46	2.19±0.45	22.6±4.6	6.57±0.46
			C = 1.5 gms./1000 gms.soln.					
$2.0x10^{-6}$	4.0	388.4	0.92±0.17	5.6±1.0	4.14±0.25	0.92±0.17	5.6±1.0	4.13±0.25
4.0	8.0	385.6	1.84±0.34	15.8±3.0	5.84±0.36	1.84±0.34	15.8±2.9	5.83±0.36
6.0	12.0	384.4	2.74±0.52	28.9±5.4	7.13±0.44	2.74±0.51	28.8±5.3	7.13±0.44
			C = 1.0 gms./1000 gms.soln.					
$2.0x10^{-6}$	4.0	405.4	0.97±0.15	6.1±0.9	4.24±0.22	0.96±0.15	6.1±0.9	4.24±0.22
4.0	8.0	402.6	1.92±0.29	16.9±2.6	5.97±0.31	1.92±0.30	16.8±2.6	5.95±0.31
6.0	12.0	401.3	2.88±0.44	30.9±4.7	7.31±0.38	2.87±0.44	30.7±4.7	7.27±0.38

molecules in the nucleus, and the size of the nucleus should be the same from a plot of $\log \tau$ versus X_c and from a plot of $\log \tau$ versus X_T. This is shown to be true in Table VI for values of $\sigma f^{2/3}$, and in Table VII for values of A, i^*f, and $h_{i^*}f^{2/3}$. The values of X_c in Table VII were arbitrarily selected within the range covered in this investigation and the values of X_T were calculated from Equation (38) as $X_T = (2.0 \times 10^6) X_c$.

The values of the activation energy presented in Table VII are dependent on the values of X_c and X_T and indicate the strong influence of supersaturation on the nucleation process. The values determined here range from 0.74 to 2.88 kcal/mole and are in the same range as the values reported by Preckshot[59] for the nucleation of potassium chloride, and as the values calculated from Chatterji and Singh's[9] work on the nucleation of potassium and ammonium halides. The values of $\sigma f^{2/3}$ in Table VI range from 5.05 to 5.39 ergs/cm^2 and are of the same order of magnitude as the corrected values of 2.5 to 4.6 ergs/cm^2 reported by Preckshot.[59] His reported values range from 1.6 to 2.9 but they are low by a factor of $2^{2/3} = 1.59$ since he neglected the factor ν in his equivalent of Equation (19). The approximate agreement between the values reported in the literature and those determined here for A and $\sigma f^{2/3}$ indicate that the calculated results presented in Tables VI and VII are the right order of magnitude.

In order to calculate values for the interfacial energy (σ), the number of molecules in the nuclei (i^*), and the size of the nuclei

(h_{i*}) it is necessary to obtain a value for the heterogeneous nucleation factor. This factor could be determined from the intercept of a plot of log τ versus X_c or X_T if all of the variables in the definition of K' were known. However, many of these variables cannot be determined. A reasonable value of f may be estimated from van Hook's statement that solid nuclei generally contain more than 100 molecules and have a characteristic dimension of the order of 10Å.(73) Assuming the nuclei formed at $X_c = 4.0 \times 10^{-6}$ to contain 100 molecules yields a value for f of approximately 0.2 which may be used to estimate the values of σ, $i*$, and h_{i*}.

The interfacial energy between calcium sulfate hemihydrate and its aqueous solution is estimated to be 13 ergs/cm^2 from the experimental data and the assumed value of 0.2 for f. This estimated value is in good agreement with the value of 15 ergs/cm^2 for calcium sulfate dihydrate reported by Deryabina and Mishchenko(16) and the value of 17 ergs/cm^2 for barium sulfate reported by Kahlweit.(34) Walton(78) reports a calculated value of 584 ergs/cm^2 for the surface energy of calcium sulfate in vacuum at $0°K$ but this value is of little use for comparison since increasing the temperature would decrease the surface energy.(45) The presence of the stainless steel and the solution would also be expected to reduce the interfacial energy.(45,53)

Calculated values of $i*$ range from 22 to 144, assuming $f = 0.2$, depending on the level of supersaturation. These values are the same order of magnitude as the value of 21 reported by Mutaftschiew

and Platikanowa[52] for calcium sulfate with $C/C_s = 6$ and the value of 200 reported by Turnbull for the solidification of mercury.[69] Values calculated for h_{i*} range from 11 to 21 Å, assuming $f = 0.2$, and are of the order of 10 Å suggested by van Hook[73] and the value of 12 Å reported by Turnbull for solid mercury.[69]

VII. SUMMARY

(1) Nucleation times were measured for the heterogeneous nucleation of calcium sulfate from unagitated aqueous solutions onto Type 316 stainless steel. Values of the nucleation time, τ, were obtained by determining the time required, after the solution had become supersaturated, for a detectable increase in the resistance of the solution which accompanies the precipitation of the calcium sulfate. These resistance changes were measured by electrical conductivity techniques using equipment capable of detecting the precipitation of the order of 10^{-7} grams of calcium sulfate.

(2) Nucleation times were measured for solution concentrations of 1.0, 1.5, 1.8, 1.9, and 2.0 grams of $CaSO_4$ per 1000 grams of solution. The temperature ranges used for these concentrations were 128.1° to 130.7°C, 111.7° to 115.7°C, 104.2° to 110.0°C, 101.9° to 107.8°C, and 101.3° to 107.8°C, respectively.

(3) The results of this nucleation study show that concentration and temperature have a strong effect on nucleation times. The temperature change required to produce a given change in the nucleation time becomes smaller as the concentration is decreased. For example, to change the nucleation time from 200 to 50 minutes requires a temperature change from 99.4° to 102.2°C (ΔT = 2.8°C) at C = 2.0 and from 127.8° to 128.8°C (ΔT = 1.0°C) at C = 1.0 grams of $CaSO_4$ per 1000 grams of solution. The change in concentration required to produce a given change in the nucleation time decreases as the temperature is increased. For example,

to change the nucleation time from 200 to 50 minutes requires changing the concentration from 1.720 to 1.815 ($\Delta C = 0.095$) at 105°C and from 1.100 to 1.126 ($\Delta C = 0.026$) at 125°C where the concentrations are expressed as grams of $CaSO_4$ per 1000 grams of solution. The corresponding changes in supersaturation, C/C_s, at these two temperatures are from 1.135 to 1.197 and from 1.120 to 1.147, respectively.

(4) The solubility of calcium sulfate hemihydrate was determined as 1.481, 1.250, and 0.885 grams of $CaSO_4$ per 1000 grams of solution at 106.0°, 114.1°, and 130.2°C, respectively. These solubilities were measured by allowing supersaturated solutions to come to equilibrium in the conductivity cells at the temperature of observation and then determining the equilibrium concentration from a knowledge of the relationship between the concentration and cell resistance. These measurements were necessary since the scatter of the solubility data in the literature would not permit a reasonable analysis of the experimental data on nucleation.

(5) The solubility study and electron diffraction patterns of some of the crystalline deposits indicate that calcium sulfate hemihydrate was the form which precipitated for the conditions used in the nucleation study.

(6) Electron micrographs of some of the crystalline deposits indicated that they were uniformly distributed on the stainless steel surface and that they did not assume a preferred orientation. The crystallites were needle-like and grew at a faster rate in the length direction than they did in the width direction.

(7) The equivalent conductivity of calcium sulfate was determined at 106.0°, 114.1°, and 130.2°C for aqueous solutions of different concentrations.

(8) Plots of log τ versus $1/T^3\log^2(C/C_s)$ and log τ versus $T_s^2/T(T-T_s)^2$ produced straight lines as predicted by theoretical equations where τ is the nucleation time, C is the concentration of the supersaturated solution, T is the temperature of observation, C_s is the saturated concentration at the temperature T, and T_s is the saturation temperature for a solution of concentration C. The slopes of these lines were independent of concentration while the intercepts decreased with decreasing concentration. The slopes of these lines were used to calculate the activation energy for nucleation, the crystal-solution interfacial energy, the characteristic size of the nuclei, and the number of molecules in the nuclei.

(9) The activation energy for nucleation depends on the degree of supersaturation and was calculated to range from 0.74 to 2.88 kcal/mole for the experimental conditions used in this study. The crystal-solution interfacial energy of calcium sulfate hemihydrate was essentially constant in this study and was estimated to be 13 ergs/cm^2. The characteristic size of the nuclei and the number of molecules in the nuclei are dependent on the degree of supersaturation and were estimated to range from 11 to 21 Å and from 22 to 144 molecules, respectively.

APPENDICES

APPENDIX A

EXPERIMENTAL DATA AND SAMPLE CALCULATIONS

The experimental data consisted of temperature, concentration, resistance, capacitance, and nucleation time. From these observed data, values were calculated for the corrected temperature, the equivalent conductivity, saturated concentration, saturation temperatures, and values of X_c and X_T. These experimental and calculated values are presented in Table A-1 with the following nomenclature and units:

T_i : Indicated temperature, °C

C : Solution concentration, gms.$CaSO_4$/1000 gms.soln.

R_4 : Resistance setting of R_4, ohms

C_4 : Capacitance setting of C_4, picofarads

τ : Nucleation time, minutes

T_c : Corrected temperature, °C

Λ : Equivalent conductivity, cm^2/ohm

C_s : Saturated concentration, gms. $CaSO_4$/1000 gms. soln.

T_s : Saturation temperature, °C

X_c : $[(T_c+273.16)^3 \log^2 (C/C_s)]^{-1} \times 10^{-6}$, $°K^{-3}$

X_T : $(T_s+273.16)^2/[(T_c+273.16)(T_c-T_s)^2]$, $°K^{-1}$

1. Calculation of T_c, Λ, C_s, T_s, X_c, and X_T

Consider Run No. 38 with cell No. 5 for which T_i = 104.00°C, C = 1.810 gms. $CaSO_4$/1000 gms.soln., and R_4 = 4636.8 ohms. From the thermometer calibrations given in Appendix B

TABLE A-1

EXPERIMENTAL AND CALCULATED DATA

Run	Cell	T_i	C	R_4	C_4	r	T_c	Λ	C_s	T_s	X_c	X_T
1	3	103.76	2.004	4056.3	702	37	104.12	160.8	1.542	93.02	1.44	2.88
2	3	103.34	2.014	4048.7	958	26	103.67	159.9	1.558	92.82	1.51	3.02
3	2	105.70	1.998	3336.1	996	28	106.23	160.6	1.470	93.15	1.03	2.06
4	3	107.21	1.976	4088.5	774	23	107.80	161.9	1.419	93.60	0.88	1.75
5	2	107.23	1.909	3440.4	956	35	107.82	163.2	1.418	95.03	1.09	2.18
6	3	103.40	1.902	4202.5	714	83	103.74	163.6	1.556	95.18	2.46	4.92
7	2	106.75	1.895	3448.6	894	53	107.32	163.9	1.434	95.34	1.24	2.48
8	3	106.71	1.900	4210.1	720	48	107.28	163.5	1.436	95.23	1.23	2.45
9	2	105.41	1.900	3459.9	894	55	105.92	162.8	1.481	95.23	1.56	3.13
10	3	105.87	1.899	4214.0	720	52	106.42	163.3	1.464	95.25	1.43	2.87
11	3	103.77	1.895	4239.9	684	56	104.14	162.3	1.542	95.34	2.32	4.65
12	2	103.54	1.897	3477.1	870	102	103.89	162.0	1.551	95.29	2.43	4.87
13	3	103.46	1.901	4229.1	678	90	103.80	162.2	1.554	95.21	2.43	4.87
14	2	101.98	1.901	3473.8	834	170	102.20	161.8	1.612	95.21	3.69	7.40
15	5	103.12	1.900	4501.0	612	67	103.43	162.0	1.567	95.23	2.67	5.35
16	3	102.91	1.901	4230.1	672	79	103.21	162.1	1.575	95.21	2.81	5.63
17	2	105.70	1.901	3458.9	804	75	106.23	162.8	1.470	95.21	1.47	2.94
18	2	105.52	1.909	3440.4	810	29	106.04	162.9	1.477	95.03	1.47	2.95
19	5	105.59	1.903	4453.6	624	34	106.11	163.8	1.474	95.16	1.49	2.98
20	3	105.52	1.905	4194.2	696	42	106.04	163.5	1.477	95.12	1.50	3.00
21	3	105.59	2.011	4030.2	750	29	106.11	161.2	1.474	92.88	1.01	2.02
22	5	105.58	2.011	4280.6	660	27	106.10	161.3	1.474	92.88	1.01	2.02
23	2	105.57	2.012	3301.3	864	22	106.09	161.1	1.475	92.86	1.01	2.02
24	5	104.51	1.998	4305.2	660	43	104.94	161.2	1.514	93.15	1.27	2.55
25	2	104.50	1.995	3331.1	840	28	104.93	160.9	1.514	93.21	1.29	2.58

TABLE A-1 (CONT'D)

Run	Cell	T_i	C	R_4	C_4	τ	T_c	Λ	C_s	T_s	X_c	X_T
26	5	103.29	1.998	4321.3	642	35	103.62	160.5	1.560	93.15	1.62	3.25
27	2	103.33	1.997	3337.7	834	47	103.66	160.2	1.559	93.17	1.61	3.23
28	4	101.20	1.997	4121.4	672	59	101.35	160.0	1.644	93.17	2.67	5.35
29	5	101.21	1.994	4344.0	636	59	101.36	159.9	1.644	93.23	2.71	5.42
30	5	101.22	2.007	4371.0	642	53	101.37	157.4	1.643	92.96	2.53	5.06
31	2	101.28	2.004	3362.2	822	74	101.43	158.0	1.641	93.02	2.52	5.05
32	3	101.28	2.011	4106.3	714	44	101.43	157.4	1.641	92.88	2.44	4.88
33	4	101.27	2.004	4138.0	648	61	101.42	158.3	1.641	93.02	2.53	5.07
34	5	105.92	1.788	4658.1	594	42	106.47	166.7	1.462	97.78	2.39	4.79
35	3	105.79	1.789	4388.1	654	66	106.33	166.4	1.467	97.75	2.46	4.93
36	4	105.88	1.790	4419.2	624	50	106.43	166.8	1.464	97.73	2.39	4.79
37	2	105.90	1.786	3597.7	756	36	106.45	166.6	1.463	97.82	2.43	4.87
38	5	104.00	1.810	4636.8	588	72	104.39	165.2	1.533	97.26	3.57	7.15
39	4	103.95	1.810	4401.2	612	97	104.33	165.4	1.535	97.26	3.63	7.26
40	4	103.94	1.842	4346.4	624	89	104.32	164.6	1.535	96.52	2.97	5.95
41	2	103.97	1.840	3532.4	768	71	104.36	164.4	1.534	96.57	2.98	5.97
42	5	109.47	1.839	4522.0	600	11	110.13	167.5	1.347	96.59	0.97	1.95
43	4	109.36	1.839	4301.7	624	20	110.02	167.3	1.351	96.59	0.99	1.98
44	3	109.36	1.809	4332.4	636	27	110.02	167.2	1.351	97.28	1.10	2.21
45	5	109.17	1.798	4617.6	588	14	109.82	167.7	1.356	97.54	1.19	2.38
46	4	109.37	1.798	4380.2	594	24	110.03	168.0	1.350	97.54	1.15	2.30
47	4	103.81	1.799	4426.3	606	68	104.18	165.4	1.540	97.52	4.09	8.20
48	3	104.08	1.800	4382.8	642	72	104.48	165.4	1.530	97.49	3.73	7.46
49	4	101.71	1.916	4271.3	624	90	101.90	160.7	1.623	94.88	3.65	7.32
50	3	101.74	1.915	4242.7	672	128	101.94	160.3	1.622	94.90	3.64	7.29

TABLE A-1 (CONT'D)

Run	Cell	T_i	C	R_4	C_4	τ	T_c	Λ	C_s	T_s	X_c	X_T
51	2	101.74	1.912	3476.3	764	127	101.94	160.5	1.622	94.97	3.71	7.43
52	5	115.17	1.497	5277.5	720	16	115.16	177.0	1.207	105.43	1.95	3.90
53	3	115.10	1.497	4974.0	690	12	115.09	176.7	1.209	105.43	1.98	3.96
54	5	112.70	1.497	5288.8	726	49	112.74	176.1	1.272	105.43	3.48	6.96
55	7	130.77	1.039	6411.0	528	15	130.66	198.3	0.875	122.21	2.71	5.43
56	4	129.58	1.039	6528.5	510	36	129.27	198.5	0.899	122.21	3.90	7.80
57	6	129.60	1.039	6168.0	534	34	129.29	198.4	0.899	122.21	3.88	7.76
58	7	128.58	1.039	6382.5	534	49	128.29	198.8	0.917	122.21	5.27	10.55
59	6	128.42	1.039	6146.7	534	118	128.13	198.6	0.920	122.21	5.55	11.12
60	4	128.48	1.039	6503.5	516	94	128.19	198.8	0.919	122.21	5.44	10.90
61	7	128.48	1.039	6369.0	534	88	128.19	199.2	0.919	122.21	5.44	10.90
62	6	128.50	1.039	6143.5	540	91	128.21	198.8	0.919	122.21	5.41	10.83
63	4	129.72	1.039	6522.0	504	32	129.40	198.7	0.897	122.21	3.75	7.51
64	7	130.71	1.039	6382.0	534	17	130.60	199.2	0.876	122.21	2.75	5.50
65	6	130.69	1.039	6157.4	534	21	130.58	198.8	0.876	122.21	2.76	5.53
66	3	112.76	1.497	4987.4	696	40	112.80	175.8	1.270	105.43	3.42	6.85
67	3	115.71	1.497	4985.0	708	14	115.68	176.0	1.193	105.43	1.75	3.51
68	5	112.68	1.497	5284.1	744	49	112.72	176.4	1.273	105.43	3.50	7.00
69	3	115.81	1.497	4986.5	714	13	115.78	175.9	1.191	105.43	1.72	3.44
70	5	112.56	1.497	5285.3	750	36	112.60	176.4	1.276	105.43	3.61	7.23
71	3	113.89	1.497	4991.3	720	20	113.90	175.6	1.240	105.43	2.58	5.16
72	5	111.62	1.497	5288.2	744	80	111.68	176.1	1.302	105.43	4.77	9.55
73	3	111.66	1.497	4991.0	726	63	111.72	175.6	1.301	105.43	4.71	9.43
74	4	128.62	1.039	6502.5	516	75	128.33	198.9	0.916	122.21	5.20	10.41
75	7	130.68	1.039	6380.5	534	14	130.57	199.3	0.876	122.21	2.77	5.54
76	6	130.73	1.039	6156.0	540	20	130.62	198.8	0.875	122.21	2.74	5.48

$$T_c = (1.0847)(104.00) - 8.42$$
$$= 112.81 - 8.42$$
$$= \underline{104.39°C}$$

The cell resistance equals R_4 since $R_1 = R_2$ and the bridge impedances may be assumed to be pure resistances as shown in Appendix E. From the solubility study the constant for cell No. 5 is found to be 19.51 cm^{-1}. In order to calculate the equivalent conductivity it is necessary to convert the concentration to equivalents per liter at 104.4°C. The molecular weight of calcium sulfate is 136.15, the specific volume of water at 104.4°C is 1.044 $cm^3/gm.$, and the solution may be assumed to have the same density as water[31] yielding

$$C' = (1.810)(2)/(136.15)(1.044)$$
$$= 0.02547 \text{ equiv./ liter}$$

Using Equation (44)

$$\Lambda = 1000\, k_c/R_c C'$$
$$= (1000)(19.51)/(4636.8)(0.02547)$$
$$= \underline{165.2\ cm^2/ohm}$$

Values of C_s and T_s may be calculated from Equation (43)

$$\log C_s = -3.5620 + (1{,}414.9)/(104.39+273.16)$$
$$= -3.5620 + 3.7476$$
$$= 0.1856$$

which yields C_s = 1.533 gms.$CaSO_4$/1000 gms.soln. By rearranging Equation (43)

$$T_s = (1{,}414.9)/(\log C + 3.5620)$$
$$= (1{,}414.9)/(0.2577 + 3.5620)$$
$$= (1{,}414.9)/(3.8197)$$
$$= 370.42°K = 97.26°C$$

Values of X_c and X_T may be calculated directly from the experimental values of C and T, the values of C_s and T_s just calculated, and the definition of X_c and X_T.

$$X_c = [(104.39+273.16)^3 \log^2 (1.810/1.533)]^{-1}$$
$$= [(377.55)^3 (0.2577-0.1856)^2]$$
$$= [(5.382 \times 10^7)(0.0721)^2]^{-1}$$
$$= (2.798 \times 10^5)^{-1} = 3.57 \times 10^{-6}\ °K^{-3}$$

$$X_T = (97.26 + 273.16)^2/(104.39+273.16)(104.39-97.26)^2$$
$$= (370.42)^2/(377.55)(7.13)^2$$
$$= (137{,}210)/(19{,}194) = 7.15\ °K^{-1}$$

2. Calculation of $\sigma f^{2/3}$, A, i^*f, and $h_{i^*f}^{2/3}$

Consider the runs made at a concentration of 2.0 gms $CaSO_4$/1000 gms.soln. for which $m_c = 2.15 \times 10^5\ °K^3$. From Equation (30) with S^j = 21f

$$\sigma f^{2/3} = (2.303R)\left[\frac{3m_c\nu^2}{84\ N_o\tilde{V}_\beta^2}\right]^{1/3}$$

$$= (2.303)(8.314\text{x}10^{7})\left[\frac{(3)(2.15\ \text{x}\ 10^{5})(2)^2}{(84)(6.023\text{x}10^{23})(52.8)^2}\right]^{1/3}$$

$$= (1.915\text{x}10^{8})(1.829\text{x}10^{-23})^{1/3}$$

$$= (1.915\text{x}10\ )(2.635\text{x}10^{-8})$$

$$= \underline{5.05\ \text{ergs/cm}^2}$$

The activation energy for the nucleation process can be calculated from Equation (34) with $X_c = 4.0\text{x}10^{-6}\ ^\circ K^{-3}$ which corresponds to a temperature of 373.1°K.

$$A = 2.303\ RT\ m_c\ X_c$$

$$= (2.303)(1.9872)(373.1)(2.15\text{x}10^{5})(4.0\text{x}10^{-6})$$

$$= 1{,}470\ \text{cal/mole} = \underline{1.47\ \text{kcal/mole}}$$

The number of molecules can be calculated from Equation (32) with $X_c = 4.0\text{x}10^{-6}\ ^\circ K^{-3}$.

$$i^*f = 2\ m_c\ (TX_c)^{3/2}/\nu$$

$$= (2)(2.15\text{x}10^{5})\ [(373.1)(4.0\text{x}10^{-6})]^{3/2}/(2)$$

$$= (2.15\text{x}10^{5})(1.492\text{x}10^{-3})^{3/2}$$

$$= (2.15\text{x}10^{5})(5.763\text{x}10^{-5}) = \underline{12.4}$$

The characteristic dimension of the nucleus can be calculated from Equation (36) with $X_c = 4.0\ \text{x}\ 10^{-6}\ ^\circ K^{-3}$ and $S^j = 21f$.

$$h_{i*}f^{2/3} = (TX_c)^{1/2} \left[\frac{6\,\tilde{V}_\beta\, m_c}{21\,\nu\, N_o}\right]^{1/2}$$

$$= \left[(373.1)(4.0\text{x}10^{-6})\right]^{1/2} \left[\frac{(6)(52.8)(2.15\text{x}10^{5})}{(21)(2)(6.02\text{x}10^{23})}\right]^{1/3}$$

$$= (1.492\text{x}10^{-3})^{1/2}\ (2.693\text{x}10^{-18})^{1/3}$$

$$= (3.863\text{x}10^{-2})(1.392\text{x}10^{-6})$$

$$= 5.38\text{x}10^{-8}\text{cm} = \underline{5.38\ \text{Å}}$$

APPENDIX B

CALIBRATION OF THERMOMETERS

Three mercury-in-glass thermometers having 0.1°C divisions were used in this investigation. The Nurnberg #4303 had a range of 50 to 110°C and was used to measure indicated temperatures from 100 to 110°C. The TCA #74312, also designated ASTM-95C, had a range of 100 to 130°C and was used to measure indicated temperatures from 110 to 130°C. The TCA #27810, also designated ASTM-96C, had a range of 120 to 150°C and was used to measure indicated temperatures above 130°C. These three thermometers were calibrated with a precision thermometer, Princo #503944, which had been certified by the National Bureau of Standards under test number G-24635. The results of these calibrations are shown in Figure B-1 and may be expressed as

$$T_c = 1.0847\ T_i - 8.42 \qquad 100 \leq T_i \leq 106$$

$$T_c = 1.0317\ T_i - 2.81 \qquad 106 \leq T_i < 110$$

$$T_c = 0.9793\ T_i + 2.37 \qquad 110 \leq T_i < 130$$

$$T_c = 0.9951\ T_i + 0.53 \qquad 130 \leq T_i < 135$$

where T_c is the corrected temperature and T_i is the indicated temperature, both in °C. These calibrations were determined with the thermometers placed in the bath in the same position that they were used throughout this investigation. The corrected temperatures are accurate within $\pm$ 0.03°C.

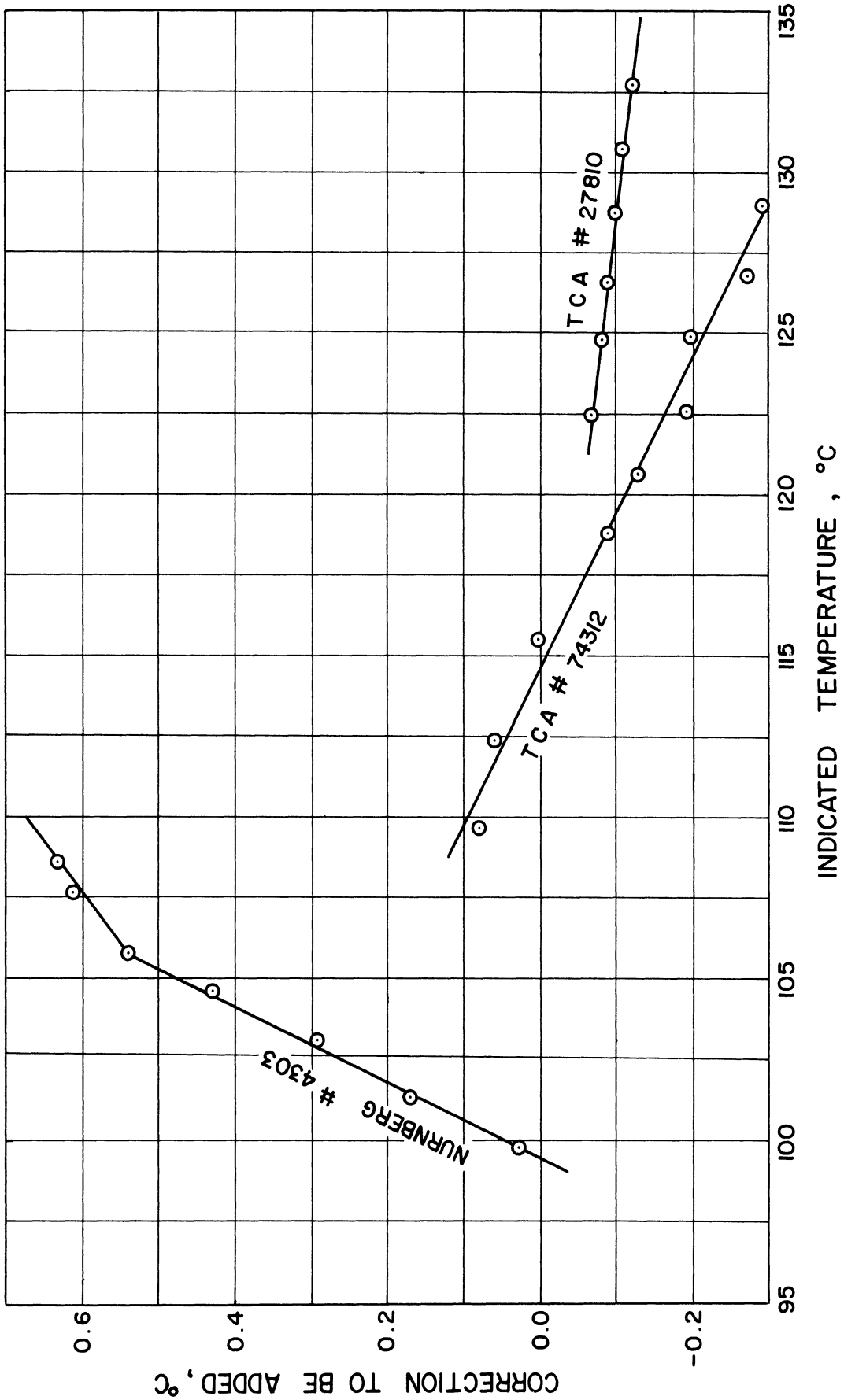

Figure B-1. Results of Thermometer Calibrations.

APPENDIX C

CALCULATION OF DETECTOR SENSITIVITY

The sensitivity of this technique for detecting nucleation may be defined as the amount of precipitated solute that can be detected and may be expressed as a mass or as a percentage of the total dissolved solute. The detectable change in cell resistance must be determined first and then related to the change in concentration.

The change in the recorded voltage which can reasonably be detected is about 0.02 millivolts at the recorder or 0.02 volts from the rectifier. Since the overall amplification of the amplifier-filter-rectifier combination is 4,000 this corresponds to a change in the output voltage of the bridge of 5.0×10^{-6} volts. Assuming a value of 4,000 ohms for R_4 and using Equation (E-5) yields

$$\Delta R_{det.} = \frac{4R_4 \Delta E_o}{E_i} \text{ det.}$$

$$= \frac{(4)(4{,}000)(5.0 \times 10^{-6})}{(17.0)}$$

$$= 4.7 \times 10^{-3} \text{ ohms}$$

Differentiation of Equation (44) with respect to C' and rearranging yields

$$\frac{dC'}{dR} = -\frac{\Lambda}{R} \cdot \frac{dC'}{d\Lambda}$$

since k_c is a constant. The change in equivalent conductivity with concentration may be determined from Figure 17 and at 106°C may be approximated as

$$\frac{dC'}{d\Lambda} \cong \frac{\Delta C'}{\Delta\Lambda} = \frac{0.02506 - 0.02098}{166.5 - 174.2}$$

$$= \frac{0.00408}{-7.7}$$

$$= -5.3 \times 10^{-4} \text{ equiv.-ohm/liter-cm}^2$$

where the values were taken from Table III. Assuming Λ to be approximately 170 cm^2/ohm yields

$$\frac{\Delta C'}{\Delta R} = \frac{(170)(5.3\times10^{-4})}{(4{,}000)} = 2.25 \times 10^{-5} \frac{\text{equiv.}}{\text{liter-ohm}}$$

Since the detectable value of ΔR is 4.7×10^{-3} ohms the detectable change in the solute concentration is given by

$$\Delta C'_{\text{det.}} = (2.25\times10^{-5})(4.7\times10^{-3}) = 1.06\times10^{-7} \text{ equiv./liter}$$

or expressed as a percentage of the solute concentration

$$\frac{\Delta C'}{C'} = \frac{1.06 \times 10^{-7}}{2.1 \times 10^{-2}} = 5.0 \times 10^{-6} = 0.0005\%$$

The cell volumes were approximately 17 cm^3 and may be used to calculate the detectable precipitation in terms of mass as

$$W = (1.06 \times 10^{-7})(17\times10^{-3})(136.15/2)$$

$$= 1.2 \times 10^{-7} \text{ gms. of } CaSO_4$$

where 136.15 is the molecular weight of calcium sulfate.

APPENDIX D

CIRCUIT DIAGRAMS FOR CONSTANT TEMPERATURE BATH AND ELECTRONIC COMPONENTS

Details are presented here on the bath heater circuits and on the circuit diagrams and operating characteristics of the amplifier, filter, and rectifier which were used in the detector.

1. Bath Heater Circuit

The circuit diagram for the bath heaters is shown in Figure D-1. The connections for the manually controlled 1000-watt heater are very simple and consist of connecting the heater, voltmeter, and ammeter to the secondary of a Variac. The connections for the automatically controlled heater require a little more explanation. In order to minimize temperature fluctations caused by the thermal lag of the control heater it was connected so that it would operate between a high and low position and never be completely turned off. The high position was set by adjusting the Variac and the low position was set relative to the high position by adjusting the 16.5 ohm rheostat. These positions were set at 70-watts and 30-watts, respectively, for all experimental work. From determinations of the heat losses from the bath at various temperatures it was possible to adjust the manual heater to make up all but about 50-watts of the heat loss so that the control heater would operate about equally in the high and low positions. The Potter-Brumfield relay was used since the electronic relay was unable to handle the switching of the inductive load presented by the secondary of the Variac. The 0.25

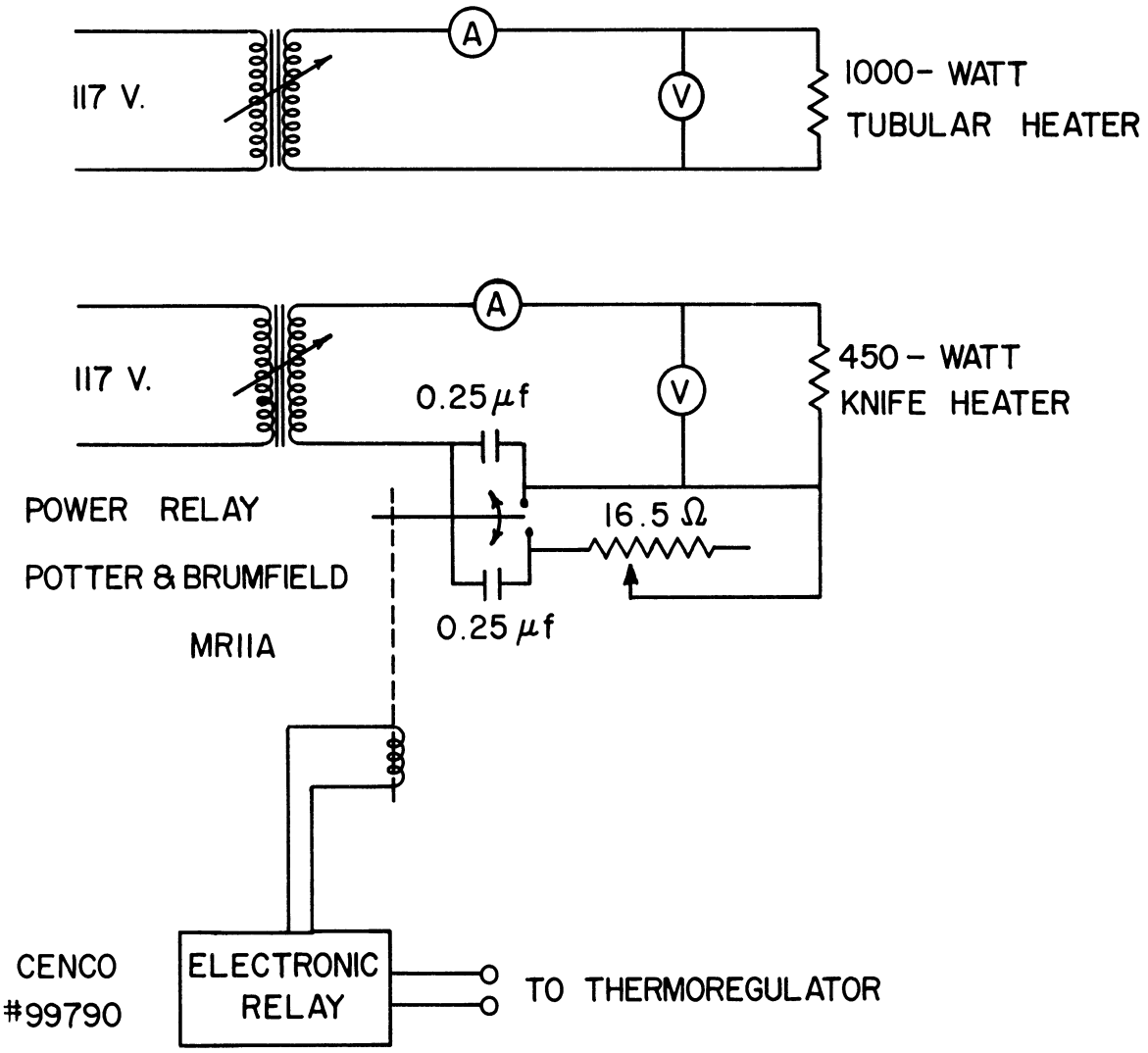

Figure D-1. Circuit Diagram of Bath Heaters.

microfarad capacitors were placed across the contacts of the DPDT relay in order to prevent serious arcing and the resulting destruction of the contacts caused by switching the inductive load. The amount of current bypassing the relay through these capacitors was negligible since they present an impedance of approximately 10,000 ohms to 60 cycle current. The power relay was operated by a sensitive electronic relay (Cenco #99790) which, in turn, was activated by a spiral bimetallic thermo-regulator (American Insturment Co., Cat. No. 4-235 F).

2. Electronic Equipment

The amplifier was a two-stage, variable gain, non-linear amplifier and is shown schematically in Figure D-2. The non-linearity was desirable in order to partially damp out 60 cycle signal picked up by the bridge. Frequency response was approximately flat from 600 to 5,000 cps with the amplification at 1,000 cps being slightly more than two times that at 60 cps. Low gain was required in order to easily maintain approximate bridge balance during the early transient part of a run, but high gain was necessary when this transient period was over in order to have high sensitivity. This variable gain was achieved by using a variable resistor to vary the signal to the grid of the second stage. The amplifier was powered by the usual transformer-rectifier-filter supply and did not introduce appreciable 60 cycle interference. The amplifier was first built with an input transformer but this was changed to the resistance-capacitance input shown in the diagram since the input transformer picked up too much 60 cycle signal.

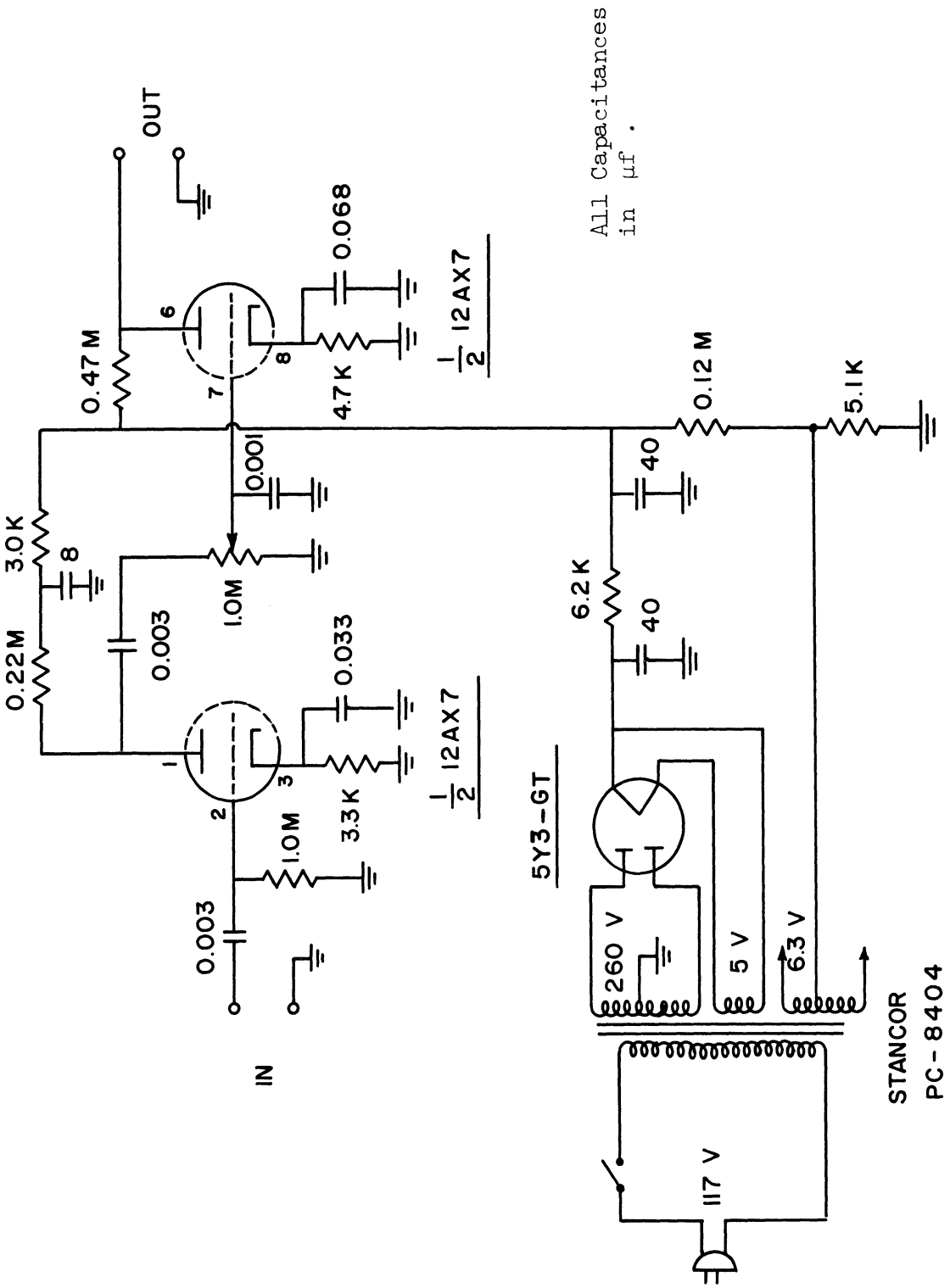

Figure D-2. Circuit Diagram of Amplifier.

The filter was a one-stage amplifier with negative feedback through a parallel-T network tuned to approximately 1000 cps, and is shown schematically in Figure D-3. This circuit is basically the same as the one used by Preckshot[59] and differs only in the values of some of the resistors. The filter was battery powered because it was convenient to do so but based on experience with the amplifier there is no reason to believe that an AC powered filter would not have worked as well. The filter differs from an ordinary pentode amplifier only by the use of negative feedback through the filter network. This network is essentially a frequency sensitive bridge tuned in such a way that when a 1000 cps signal is applied to point A no signal will appear at B but the more the signal at A deviates from 1000 cps the larger will be the signal appearing at B .[65] Since the signal produced at B is 180° out of phase with the signal applied to the control grid it reduces the amplification of signals differing from 1000 cps, and the greater the deviation from this frequency the greater the reduction of the signal.

The rectifier was a one stage amplifier with a cathode follower, full wave rectifier, and a resistance-capacitance filter as shown by the circuit diagram of Figure D-4. This was a modified version of a similar instrument reported by Clements and Schnelle.[10] Amplification was provided by one triode section while the second triode section was connected as a cathode follower impedance transformer which prevented excess loading of the amplifier section by the voltage

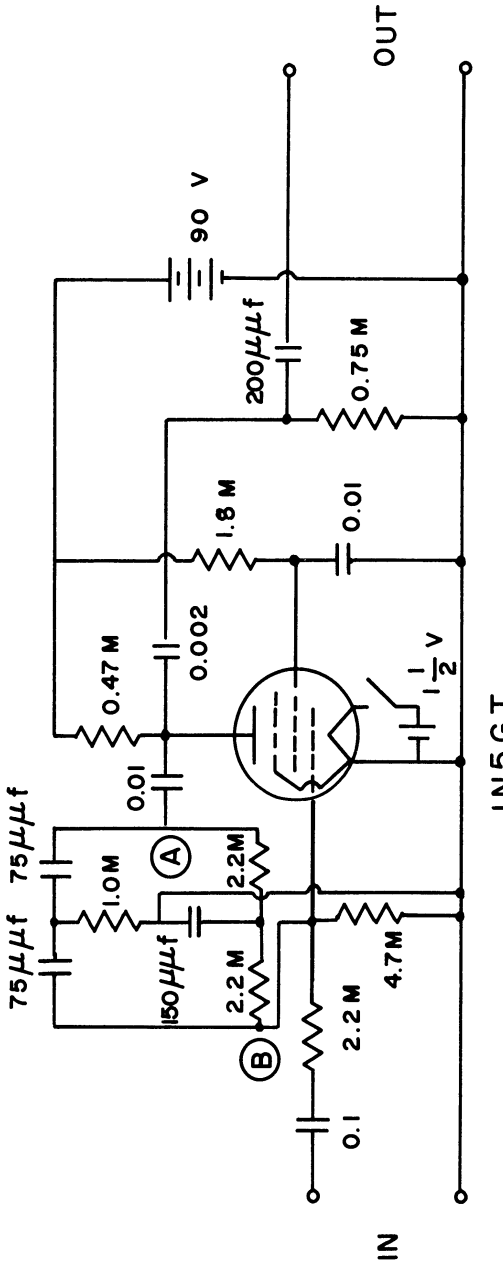

Capacitances in μf
unless noted otherwise.

Figure D-3. Circuit Diagram of Filter.

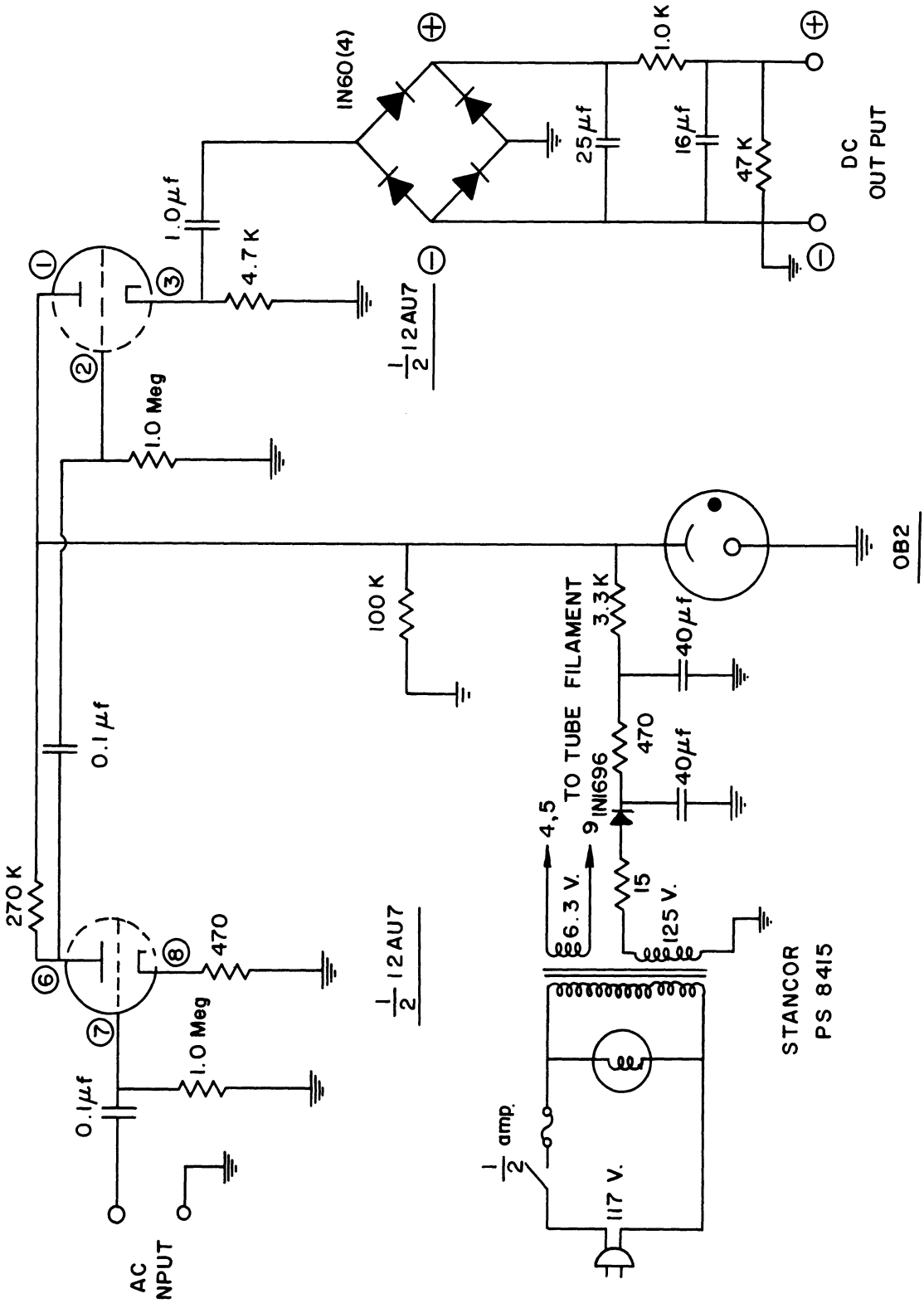

Figure D-4. Circuit Diagram of Rectifier.

divider. The 1000 cps signal was rectified by the diode bridge and filtered by a resistance-capacitance network. No ripple could be detected when the rectified output voltage was examined on a Hewlett-Packard 130BR oscilloscope at a sensitivity of 1 millivolt per centimeter.

APPENDIX E

CALCULATION OF BRIDGE OUTPUT VOLTAGE

The effects of capacitance on the balanced values of the resistors in the AC bridge and the change in the output voltage of the bridge with a change in the cell resistance are developed in this appendix.

Consider the bridge shown in Figure E-1 which is the same circuit as the bridge in Figure 3 with the conductivity cell replaced by R_3 and C_3. This is a reasonable substitution since the principal capacitance of a cell is in parallel with the cell resistance.[22,23] Using impedances, the relation between the output voltage (E_o) and the input voltage (E_i) is given by

$$\frac{E_o}{E_i} = \frac{Z_1 \cdot Z_3 - Z_2 \cdot Z_4}{(Z_1+Z_2)(Z_3+Z_4)} \qquad \text{(E-1)}$$

where each of these components are phasors. Equation (E-1) assumes an infinite impedance across the output terminals which is approximated for all practical purposes by the 1 megohm input resistor of the amplifier. At balance $E_o = 0$ or

$$Z_1 \cdot Z_3 = Z_2 \cdot Z_4$$

or in terms of magnitudes and phase angles

$$|Z_1| \cdot |Z_3| = |Z_2| \cdot |Z_4|$$

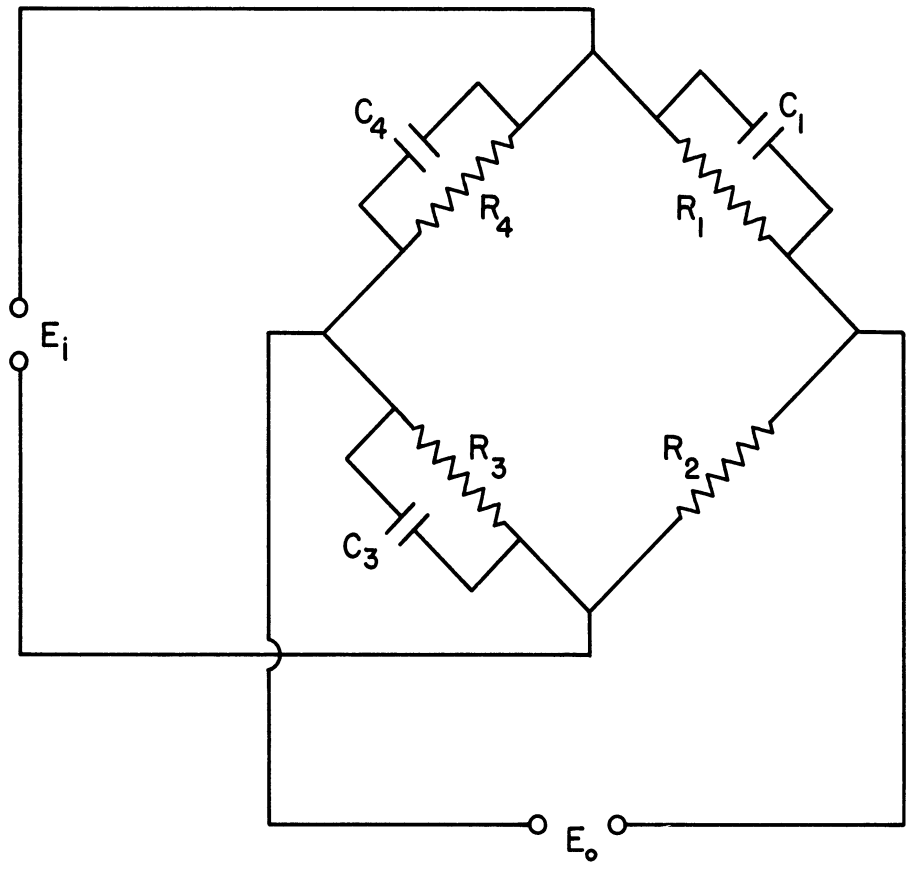

Figure E-1. Equivalent of Bridge Used in Nucleation Study.

and

$$\theta_1 + \theta_3 = \theta_2 + \theta_4$$

For the bridge being considered

$$Z_1 = \frac{R_1(1-j\omega R_1 C_1)}{1 + (\omega R_1 C_1)^2}$$

$$Z_2 = R_2$$

$$Z_3 = \frac{R_3(1-j\omega R_3 C_3)}{1 + (\omega R_3 C_3)^2}$$

$$Z_4 = \frac{R_4(1-j\omega R_4 C_4)}{1 + (\omega R_4 C_4)^2}$$

which yields

$$|Z_1| = \frac{R_1}{\sqrt{1 + (\omega R_1 C_1)^2}} \qquad \theta_1 = -\tan^{-1}(\omega R_1 C_1)$$

$$|Z_2| = R_2 \qquad \theta_2 = 0$$

$$|Z_3| = \frac{R_3}{\sqrt{1 + (\omega R_3 C_3)^2}} \qquad \theta_3 = -\tan^{-1}(\omega R_3 C_3)$$

$$|Z_4| = \frac{R_4}{\sqrt{1 + (\omega R_4 C_4)^2}} \qquad \theta_4 = -\tan^{-1}(\omega R_4 C_4)$$

R_4 ranged from 3,500 to 6,500 ohms and C_4 ranged from 500 to 1000 picofarads, R_1 was set at 3,500 or 5,000 ohms, and C_1 was constant at 476 picofarads for all of the experimental work. The largest error in neglecting the capacitances when calculating the impedances is when the resistance and capacitance are the largest.

Using the above values

$$(\omega R_1 C_1)^2_{max} = [(2\pi)(1,000)(5,000)(476\times10^{-12})]^2 = 2.24 \times 10^{-4}$$

$$\sqrt{1.000224} = \underline{1.000112}$$

$$(\omega R_4 C_4)^2_{max} = [(2\pi)(1,000)(6,500)(1,000\times10^{-12})]^2 = 4.17 \times 10^{-4}$$

$$\sqrt{1.000417} = \underline{1.000208}$$

This last figure is too large since the high values of R_4 correspond to the low concentration-high temperature runs for which the values of C_4 were the lowest. At any rate, it is safe to say that assuming the impedances to be pure resistances introduces an error of less than 0.02% in calculating the conductivities in Table A-1 or in the solubility determinations.

Having shown that the impedances may be assumed to be pure resistances Equations (E-1) may be rewritten as

$$\frac{E_o}{E_i} = \frac{R_1R_3 - R_2R_4}{(R_1+R_2)(R_3+R_4)} \qquad (E\text{-}2)$$

For the case where $R_1 = R_2$, as was done throughout this study, Equation (E-2) becomes

$$\frac{E_o}{E_i} = \frac{R_3 - R_4}{2(R_3+R_4)} \qquad (E\text{-}3)$$

Equation (E-3) explains why it is necessary to keep R_4 less than R_3 if an increase in R_3 is to cause an increase in the magnitude of E_o.

In order to see how the bridge output voltage changes with a change in R_3 let R_3 change by an amount ΔR and use Equation (E-3) twice to obtain

$$\frac{\Delta E_o}{E_i} = \frac{R_3+\Delta R-R_4}{2(R_3+R_4+\Delta R)} - \frac{R_3 - R_4}{2(R_3+R_4)} \qquad (E\text{-}4)$$

Equation (E-4) may be simplified by two assumptions: (1) ΔR is negligible compared to $R_3 + R_4$, and (2) R_3 is nearly equal to R_4. With these assumptions Equation (E-4) becomes

$$\frac{\Delta E_o}{E_i} = \frac{\Delta R}{4R_4} \qquad (E\text{-}5)$$

Equation (E-5) may be used to calculate the change in the output voltage of the bridge in terms of the input voltage, the value of R_4, and the change in R_3.

APPENDIX F

LIST OF MAJOR EQUIPMENT

Constant Temperature Bath

Container:

Precision Scientific Company
Catalog No. 10192
Serial No. G-12

Thermoregulator:

American Insturment Company
Catalog No. 4-235F
Sensitivity 0.005°C

Electronic Relay:

Central Scientific Company
Catalog No. 99790

Power Relay:

Potter & Brumfield
Type MR11A

Beckman Thermometer:

Kahlsico
#60-956
Range: -0.2 to +6.2°C, 0.01°C div.

Thermometer:

Nurnberg
#4303
Range: 50 to 110°C, 0.1°C div.

Thermometer:

Thermometer Corporation of America
#74312
Range: 100 to 130°C, 0.1°C div.
ASTM - 95C

Thermometer:

Thermometer Corporation of America
#27810
Range: 120 to 150°C, 0.1°C div.
ASTM - 96C

Oscillator

Hewlett-Packard Company
Model 200 CD
Serial No. 229-41351

Bridge

Capacitor C_1:

Western Electric Company
Fixed capacitor, 476 picofarads

Capacitor C_4:

General Radio Company
Type 222-S
Serial No. 207
Range: 50 to 3000 picofarads

Resistor R_1:

General Radio Company
Type 1432-N
Serial No. 39093
Range: 0 to 11,111 ohms, 0.1 ohm steps

Resistor R_2:

Leeds & Northrup Company
Catalog No. 4748
Serial No. 716389
Range: 0 to 11,110 ohms, 1 ohm steps

Resistor R_4:

General Radio Company
Type 1432-N
Serial No. 39091
Range: 0 to 11,111 ohms, 0.1 ohm steps

Grounding Circuit

Capacitor C_6:

Radio Condenser Company
Range: 15-370 picofarads

Resistor R_5:

Heath Company
Model DR-1
Range: 0 to 99,999 ohms, 1 ohm steps

Resistor R_6:

Heath Company
Model DR-1
Range: 0 to 99,999 ohms, 1 ohm steps

Detector

Oscilloscope:

Hewlett-Packard Company
Model 130BR
Serial No. 001-04168

Voltage Divider:

Leeds & Northrup Company
Catalog No. 2166
Serial No. 559432

Recorder:

Minneapolis-Honeywell
Model No. Y153C64(P4)-(228)-42(L)(V)
Serial No. 795637

REFERENCES

1. Akhumov, E. I. and Rozen, B. Ya., "The Second Curve of Solubility (Supersaturation)," Doklady Akad. Nauk S.S.S.R., 85, 363-6(1952), C.A., 48, 4936f (1954).

2. Amsler, J., "Nucleus Formation in Supersaturated Solution," Helv. Phys. Acta, 15, 699-732 (1942).

3. Babayan, S. G., Pakhomov, B. G., Melikhov, I. V., and Merkulova, M. S., "Method of Investigating the Crystallization Kinetics of Supersaturated Solutions," Radiochemistry, 3, 136 (1962).

4. Badger, W. L. and Banchero, J. T., "Symposium on Saline Water Conversion," Publication 568, National Academy of Sciences-National Research Council, Washington, D. C., 1962, pp. 44-50.

5. Banchero, J. T. and Gordon, K. F., "Scale Deposition on a Heated Surface," Saline Water Conversion, Advances in Chemistry Series, No. 27, American Chemical Society, Washington, D. C., 1960, pp. 105-14.

6. Becker, R. and Doering, W., "The Kinetic Treatment of Nuclear Formation in Supersaturated Vapors," Ann. Phys., 24, 719-52 (1935).

7. Campbell, W. B., "An Inexpensive Pyrex Conductivity Cell," J. Am. Chem. Soc., 51, 2419-20 (1929).

8. Caspari, W. A., "Calcium Sulphate Hemihydrate and the Anhydrites. I. Crystallography," Proc. Royal Soc. London, A155, 41-8 (1936).

9. Chatterji, A. C. and Singh, R. N., "Nucleation from Quiet Supersaturated Solutions of Alkali Halides. Part I. Potassium and Ammonium Chlorides, Bromides, and Iodides," J. Phys. Chem., 62, 1408-11 (1958).

10. Clements, W. C., Jr. and Schnelle, K. B., Jr., "Electrical Conductivity in Dynamic Testing," ISA Journal, 10, 63-8 (1963).

11. Cywin, A., "Symposium on Saline Water Conversion," Publication 568, National Academy of Sciences -- National Research Council, Washington, D. C., 1958, pp. 29-34.

12. Daniels, F., Mathews, J. H., Williams, J. W., Bender, P., and Alberty, R. A., Experimental Physical Chemistry, 5th ed., McGraw-Hill Book Company, Inc., New York, 1956, pp. 113-4.

13. Davies, C. W. and Jones, A. L., "The Precipitation of Silver Chloride from Aqueous Solutions," Disc. Faraday Soc., 5, 103-11 (1949).

14. de Coppet, L. C., "Researches on Supercooling and Supersaturation," Ann. chim. et phys., 10, 457-527 (1907), C. A., 1, 1819 (1907).

15. Dehlinger, U. and Wertz, E., "Nucleus Formation in Aqueous Solutions," Ann. Physik, 39, 226-40 (1941).

16. Deryabina, N. V. and Mishchenko, K. P., "Rate of Crystallization of Calcium Sulfate from Water Solutions of Various Salts," Problemy Kinetiki i Kataliza, 7, Statist. Yavleniya v Geterogen. Sistem., Akad. Nauk. S.S.S.R., 123-36 (1949), C. A., 48, 13334b (1954).

17. "Desalination Research and the Water Problem," Publication 941, National Academy of Sciences -- National Research Council, Washington, D. C., 1962.

18. Dufour, L. and Defay, R., Thermodynamics of Clouds, Academic Press, New York, 1963.

19. Dundon, M. and Mack, E., "The Solubility and Surface Energy of Calcium Sulfate," J. Am. Chem. Soc., 45, 2479-2485 (1923).

20. Dunning, W. J., "Theory of Crystal Nucleation from Vapor, Liquid, and Solid Systems," Chemistry of the Solid State, W. E. Garner, ed., Academic Press, New York, 1955, pp. 159-83.

21. Fletcher, N. H., "Size Effect in Heterogeneous Nucleation," J. Chem. Phys., 29, 572-6 (1958).

22. Glasstone, S., An Introduction to Electrochemistry, D. Van Nostrand Company, Inc., Princeton, N. J., 1946.

23. Glasstone, S., Textbook of Physical Chemistry, D. Van Nostrand Company, Inc., Princeton, N. J., 1946.

24. Gordon, K. F. and Smith, G. C., "Initiation and Growth of Scale on a Heated Surface," Dechema Monograph., 47, 192-205 (1962).

25. Hall, R. E., Robb, J. A., and Coleman, C. E., "The Solubility of Calcium Sulfate at Boiler-Water Temperatures," J. Am. Chem. Soc., 48, 927-38 (1926).

26. Hartley, H. and Barrett, W. H., "Sodium Sulphite and Its Equilibrium with Water," J. Chem. Soc., 95, 1178-85 (1909).

27. Hartley, H., Jones, B. M., and Hutchinson, G. A., "The Spontaneous Crystallization of Sodium Sulphate Solution," J. Chem. Soc., 93, 825-33 (1908).

28. Hillier, H., "Scale Formation in Sea Water Distilling Plants and Its Prevention," Inst. Mech. Engrs. (London) Proc., 1B, 295-311 (1952).

29. Hirth, J. P. and Pound, G.M., "Condensation and Evaporation. Nucleation and Growth Kinetics," Progess in Materials Science, 11, B. Chalmers, ed., Macmillan, New York, 1963.

30. Hollomon, J. H. and Turnbull, D., "Nucleation," Progress in Metal Physics, 4, B. Chalmers and R. King, eds., Pergamon Press, London, 1953, pp. 333-388.

31. Hulett, G. A. and Allen L. E., "The Solubility of Gypsum," J. Am. Chem. Soc., 24, 667-79 (1902).

32. International Critical Tables, Vol. 6, McGraw-Hill Book Company, Inc., New York, 1929.

33. Jones, B. M., "Spontaneous Crystallization of Solutions of Sodium Carbonate and Sodium Thiosulphate," J. Chem. Soc., 95, 1672-82 (1909).

34. Kahlweit, M., "Kinetics of Phase Formation in Condensed Systems, (Precipitation of Difficultly Soluble Electrolytes from Aqueous Solutions)," Z. Physik. Chem., 25, 125 (1960), C. A., 54, 23654i (1960).

35. Kay, D., Techniques for Electron Microscopy, Blackwell Scientific Publications, Oxford, 1961.

36. Klotz, I. M., Chemical Thermodynamics, Prentice-Hall, Inc., New York, 1950.

37. Kornfeld, G., "Overstepping Phenomena. Undercooling," Monatsh. Chem., 37, 609 (1916), C. A., 11, 734 (1917).

38. LaMer, V. K. and Dinegar, R. H., "The Limiting Degrees of Supersaturation of the Sparingly Soluble Sulfates," J. Am. Chem. Soc., 73, 380-5 (1951).

39. Langelier, W. F., Caldwell, D. H., Lawrence, W. B., and Spaulding, C.H., "Scale Control in Sea Water Distillation Equipment," Ind. Eng. Chem., 42, 126-30 (1950).

40. Lewis, G. N. and Randall, M., Thermodynamics, 2nd, ed., McGraw-Hill Book Company, Inc., New York, 1961, pp. 227-8.

41. Luder, W. F., "The Precision Conductivity Bridge Assembly," J. Am. Chem. Soc., 62, 89-95 (1940).

42. Marshall, W. L., Slusher, R., and Jones, E. V., "Aqueous Systems at High Temperature. XIV. Solubility and Thermodynamic Relationships for $CaSO_4$ in NaCl-H_2O Solutions from 40° to 200°C, 0 to 4 molal NaCl," J. Chem. Eng. Data, 9, 187-91 (1964).

43. Matuno, Y., Koganemaru, T., and Hara, R., "Calcium Sulfate in Sea Water as an Element of Boiler Incrustation," J. Soc. Chem. Ind., Japan 44, 74-6 (1941).

44. McIlhenny, W. F., "Minimizing Scale Formation in Saline Water Evaporators," Saline Water Conversion -- II, Advances in Chemistry Series, No. 38, American Chemical Society, Washington, D. C., 1963, pp. 40-51.

45. Michaels, A. S., "Fundamentals of Surface Chemistry and Surface Physics," Symposium on Properties of Surfaces, ASTM Special Technical Publication No. 340, 3-23 (1963).

46. Miers, H. A., "The Birth and Affinities of Crystals," Engineering, 83, 555-6 (1907).

47. Miyauchi, T. and Moriyama, T., "Control of Calcium Sulfate Concentration in Sea-Water Evaporator Seeded with Anhydrous Calcium Sulfate Crystals," Kagaku Kogaku, 25, 460-8 (1961), trans. J. Chen.

48. Miyauchi, T. and Moriyama, T., "Rate of Anhydrous $CaSO_4$ Scale Formation in Sea-Water Evaporators," Kagaku Kogaku, 25, 531-8 (1961), trans. J. Chen.

49. Moriyama, T. and Utsunomiya, T., "Rate of Decrease of Concentration of Supersaturated Calcium Sulfate Solution due to Spontaneous Nucleation," Kogyo Kagaku Zasshi, 60, 1268-71 (1957), trans. J. Chen.

50. Moriyama, T. and Utsunomiya, T., "Scale Prevention in Sea Water Evaporator. I. The Rate of Crystal Growth of $CaSO_4 \cdot 2H_2O$ and $CaSO_4$," Asahi Garasu Kenkyu Hokoku, 7, 69-82 (1957), trans. J. Chen.

51. Mullin, J. W., Crystallization, Butterworths, London, 1961.

52. Mutaftschiew, B. and Platikanowa, W., "Kinetics of Nucleation in Solutions," Compt. Rend. Acad. Bulgare Sci., 14, 695-8 (1961), C. A., 57, 7991a (1962).

53. Newkirk, J. B. and Turnbull, D., "Nucleation of Ammonium Iodide Crystals from Aqueous Solutions," J. Appl. Phys., 26, 579-83 (1955).

54. Ostwald, W. "Studies on the Growth and Transformation of Solid Bodies," Z. physik. Chem., 22, 289-98 (1897).

55. Partridge, E. P., "Formation and Properties of Boiler Scale," Engineering Research Bulletin No. 15, Dept. of Engineering Research, Univ. of Michigan, Ann Arbor, June, 1930.

56. Partridge, E. P., and White, A. H., "Solubility of Calcium Sulfate from 0° to 200°," J. Am. Chem. Soc., 51, 360-70 (1929).

57. Posnjak, E., "The System, $CaSO_4$ -- H_2O ," Am. J. Sci., 235A, 247-72 (1938).

58. Power, W. H., Fabuss, B. M., and Satterfield, C. N., "Transient Solubilities in the Calcium Sulfate -- Water System," J. Chem. Eng. Data, 9, 437-42 (1964).

59. Preckshot, G. W., "The Effect of Some Ionic Crystals in Nucleating Quiet Supersaturated Potassium Chloride Solutions," Ph. D. Thesis, Univ. of Michigan, Ann Arbor, 1951

60. Riddell, W. C., cited by Kelley, K. K., Southard, J. C., and Anderson, C. T., "Thermodynamic Properties of Gypsum and Its Dehydration Products," U. S. Bureau of Mines Tech. Paper No. 625, 1941.

61. Schaefer, V. J., "The Production of Ice Crystals in a Cloud of Supercooled Water Droplets," Science, 104, 457-64 (1946).

62. Schierholtz, O. J., "The Crystallization of Calcium Sulfate Dihydrate," Can. J. Chem., 36, 1057-63 (1958).

63. Shedlovsky, T., "A Screened Bridge for the Measurement of Electrolytic Conductance. I. Theory of Capacitance Errors. II. Description of the Bridge," J. Am. Chem. Soc., 52, 1793-1805 (1930).

64. Simizu, K., "Sea Water Concentration. 2. Scale," Kagaku Kogaku, 25, 251-9 (1961), trans. J. Chen.

65. Stout, M. B., Basic Electrical Measurements, Prentice-Hall, Englewood Cliffs, N. J., 1950.

66. Sugimoto, K., Irie, K., and Funaoka, M., "Synthetic Gypsum obtained by the Reaction between Waste Liquor from the Distiller of an Ammonia Soda Plant and Glauber's Salt Solution. II. Growth of Gypsum Crystals without Adding Organic Acid," Asahi Garasu Kenkyu Hokoku, 3, 205-15 (1953), trans. J. Chen.

67. Tamman, G., The States of Aggregation, trans. R. F. Mehl, D. Van Nostrand Company, New York, 1925.

68. Ting, H. H. and McCabe, W. L., "Supersaturation and Crystal Formation in Seeded Solutions," Ind. Eng. Chem., 26, 1201-7 (1934).

69. Turnbull, D., "Kinetics of Solidification of Supercooled Liquid Mercury Droplets," J. Chem. Phys., 20, 411-24 (1952).

70. Turnbull, D., "The Kinetics of Precipitation of Barium Sulfate from Solution," Acta Met., 1, 684-91 (1953).

71. Turnbull, D., "Phase Changes," Solid State Physics, 3, F. Seitz and D. Turnbull, eds., Academic Press, New York, 1956, pp. 225-306.

72. Turnbull, D. and Fisher, J. C., "Rate of Nucleation in Condensed Systems," J. Chem. Phys., 17, 71-3 (1949).

73. Van Hook, A., Crystallization: Theory and Practice, Reinhold Publishing Corp., New York, 1961.

74. Volmer, M., Kinetics of Phase Formation, Theodor Steinkopf, Dresden and Leipzig, trans. U. S. Intelligence Department, A.T.I. 81935, Central Air Documents Office, Wright-Patterson AFB, Dayton, Ohio, 1939.

75. Volmer, M., "Particle Formation and Particle Action as a Special Case of Heterogeneous Catalysis," Z. Electrochem., 35, 555-61 (1929).

76. Volmer, M. and Weber, A., "Nucleus Formation in Supersaturated Systems," Z. physik. Chem., 119, 277-301 (1926).

77. Walton, A. G., "Nucleation and Interfacial Tension of Sparingly Soluble Salts," Mikrochim. Acta, 29, 422-30 (1963).

78. Walton. A. G. and Whitman, D. R., "Calculation of the Surface Energy for Some Orthorhombic Sulfates," J. Chem. Phys., 40, 2722-4 (1964).

79. Wells, A. F., "Crystal Growth," Ann. Repts. on Progress Chem., 43, 62-87 (1946).

80. White, M. L., "Nucleation of Supersaturated Potassium Nitrate Solutions," Ph. D. Thesis, Northwestern Univ., Evanston, Ill., 1953.

81. Willard, H. H., Furman, N. H., and Bricker, C. E., Elements of Quantitative Analysis, D. Van Nostrand Company, Inc., Princeton,N.J., 1956.

82. Williamson, A. T., "The Exact Calculation of Heats of Solution from Solubility Data," Trans. Faraday Soc., 40, 421-36(1944).

83. Young, S. W., "Mechanical Stimulus to Crystallization in Supercooled Liquids," J. Am.Chem. Soc., 33, 148-54 (1911).